Article:
Yang, Z, Li, K orcid.org/0000-0001-6657-0522, Niu, Q et al. (1 more author) (2017) A novel parallel-series hybrid meta-heuristic method for solving a hybrid unit commitment problem. Knowledge-Based Systems, 134. pp. 13-30. ISSN 0950-7051

https://doi.org/10.1016/j.knosys.2017.07.013

A novel parallel-series hybrid meta-heuristic method for solving a hybrid unit commitment problem

Zhile Yang[a], Kang Li[a], Qun Niu[b], Yusheng Xue[c]

[a] *School of Electronics, Electrical Engineering and Computer Science, Queen's University Belfast, Belfast, BT9 5AH, United Kingdom (Email:yangzhile@hotmail.com,k.li@qub.ac.uk).*
[b] *School of Mechatronic Engineering and Automation, Shanghai Key Laboratory of Power Station Automation Technology, Shanghai University, Shanghai 200072, China (Email: comelycc@hotmail.com)*
[c] *State Grid Electric Power Research Institute, 210003, Jiangsu, China (Email: xueyusheng@sgepri.sgcc.com.cn)*

Abstract: Unit commitment is a traditional mixed-integer non-convex problem and remains a key optimisation task in power system scheduling. The high penetration of intermittent renewable generations such as wind and solar as well as mass roll-out of plug-in electric vehicles (PEVs) impose significant challenges to the traditional unit commitment problem, not only by significantly increasing the complexity of the problem in terms of the dimension and constraints, but also dramatically change the problem formulation. In this paper, a new hybrid unit commitment problem considering renewable generation scenarios and charging and discharging management of plug-in electric vehicles is first formulated. To effectively solve the problem, a novel parallel-series hybrid meta-heuristic optimisation method is then proposed, which combines a hybrid topology binary particle swarm optimisation, the self-adaptive differential evolution algorithm and a lambda iteration method, to simultaneously and intelligently determine the binary on/off status of each thermal unit, the generation power of online units, as well as the demand side management of plug-in electric vehicles. The proposed parallel-series hybrid method is first assessed on a 10-unit benchmark, and then on a case where renewable generation and smart PEV management are integrated. Numerical results confirm the superiority of the proposed new algorithm in comparison with some popular meta-heuristic approaches.

Keywords: unit commitment, hybrid meta-heuristic optimisation, binary particle swarm optimisation, differential evolution, renewable generation, plug-in electric vehicles

1. Introduction

Unit commitment (UC) is a crucial component of the power system operation, which aims to minimise the economic cost considering the physical system limits. A small improvement in the optimisation like 0.5% would bring millions of dollars cost reduction per year for a large utility grid [1]. The UC problem is a non-convex mix-integer optimisation problem in which both the number of discrete and continuous variables increases exponentially as the power system scale increases, leaving the UC problem remain to be a significant challenging task. Numerous computational methods have been proposed for solving the UC problems. Conventional methods, such as priority list [2,3], dynamic programming [4], Branch and Cut algorithm [5] and Lagrangian Relaxation [6], can efficiently produce a reasonable good solution but often encounter difficulties when the dimensionality of the problem increases or the problem becomes highly non-linear and non-convex. Intelligent methods have been widely employed to solve the UC and other engineering optimisation problems [7,8] including simulated annealing (SA) [9], genetic algorithm (GA) [10,11], particle swarm optimisation (PSO) [12,13], gravitational search algorithm (GSA) [14], invasive weed optimisation [15], and some other methods [16]. Some hybrid methods are also proposed using evolutionary programming (EP) [17] and EA [18] to update the Lagrangian multipliers in the Lagrangian Relaxation. However, aforementioned intelligent and hybrid methods often suffer from slow convergence due to the excessive number of iterations and mixed-integer nature of the problem. To balance the optimisation speed and the exploitation ability, binary intelligent optimisations such as binary PSO (BPSO) [19,20], quantum-inspired evolutionary algorithms (QEA) [21] and quantum-inspired binary gravitational search algorithm (QGSA) [22] have been combined with lambda iteration method to solve the problem in two stages. Though a number of researches have been carried out, the traditional UC problem has become even more challenging due to the large penetration of renewable energy generations (REG) [23] and mass roll-out of plug-in electric vehicles (PEVs) [24], all these call for more powerful tools for solving the non-convex nonlinear mixed-integer high-dimensional problem.

Among various recent developments in decarbonising the whole energy chain, transportation electrification is a key measure to reduce global dependency on fossil fuels. It is also a promising solution to reduce green-house gas emissions and other air pollutants such as NO_x and SO_x produced by internal combustion engines [25], especially given the ambitious target to limit the maximum temperature rise within 2^{o}C by the end of this

century in the recent global agreement, forged in 2015 Paris Climate Conference [26]. Electric vehicles (EVs) use electric motors to partly or completely replace the ICE and therefore see low or no fossil fuel consumption as well as reduced tailgate emissions [27]. There are three main types of EVs including pure battery electric vehicles (BEVs), hybrid electric vehicles (HEVs) (mainly referring to the none-plug-in EVs), as well as plug-in hybrid electric vehicles (PHEVs), where both BEV and PHEV are referred as PEVs [28]. On one hand, the increasing penetration of PEVs significantly challenges the existing power system operation strategy and facility [29]. On the other hand, the large capacities of PEV batteries provide possibilities to vehicle to grid (V2G) power feeding back [30] and other ancillary services such as frequency regulation [31], power reserve [32] and increase renewable energy power penetration [33,34,35]. Meanwhile, the energy flow management of individual PEVs is fundamental in supporting ancillary services and improving energy efficiency [36,37,38,39,40,41]. From the system operator perspective, different PEV coordinated scheduling strategies have shown significant impact on the economic and environmental cost [42,43,44]. In the references [45,46], the original UC problem and the integer numbers of PEVs which are charged and discharged in each hour for one day horizon are optimised together by binary and integer PSO methods. Generally speaking, the intelligent charging and discharging dispatch of PEVs in day-ahead power system scheduling is a typical load shaping demand side management (LSDSM) [47,48] and a crucial technique to level load curve and improve energy efficiency [49]. Very few publications however have paid attention to the development of mathematical tools to simultaneously solve the UC problem associated with the LSDSM of PEVs.

The main contributions of this paper are summarised below:

1. A new hybrid unit commitment problem, namely hybrid unit commitment (HUC) is formulated, which integrates the traditional unit commitment problem with demand side management of PEV charging/discharging and renewable generations.
2. A novel parallel-series hybrid meta-heuristic optimisation method (PSH) algorithm structure is proposed by integrating a new hybrid topology binary PSO (HTBPSO), self-adaptive differential evolution algorithm (SaDE) and the lambda iteration method which can effectively solve the complex and challenging HUC problem.

3. A double-priority-list method is proposed to provide priority sequence for both unit commitment and PEV charging/discharging dispatch.
4. Extensive simulation studies are conducted to assess the superb performance of the proposed PSH method.

The rest of this paper is organised as follows: Section 2 proposes the HUC problem formulation. Preliminaries for the PSH meta-heuristic method are presented in Section 3. Section 4 details the implementation procedure of the proposed PSH method in solving the HUC problem. Two cases including the original 10-unit UC problem and UC problem integrated with wind power and PV power generations as well as intelligent PEVs scheduling are comparatively studied in Section 5; Section 6 summarises and concludes the paper.

2. Problem formulation

The new HUC problem is formulated on the conventional UC basis, which is integrated with renewable wind and solar power generations and PEV aggregator as shown in Figure 1. The power flow from grid to users is denoted as red solid and dash lines (colour edition) and the power flow from generation to grid is shown as blue lines. The renewable energy generation is undispatchable due to the intermittent nature and assumed to be fully accepted into the grid. The traditional power demand considered in this paper is assumed to be non-controllable, while the PEV aggregator is a controllable demand, which coordinates all the PEV charging and discharging behaviours and plays the LSDSM role.

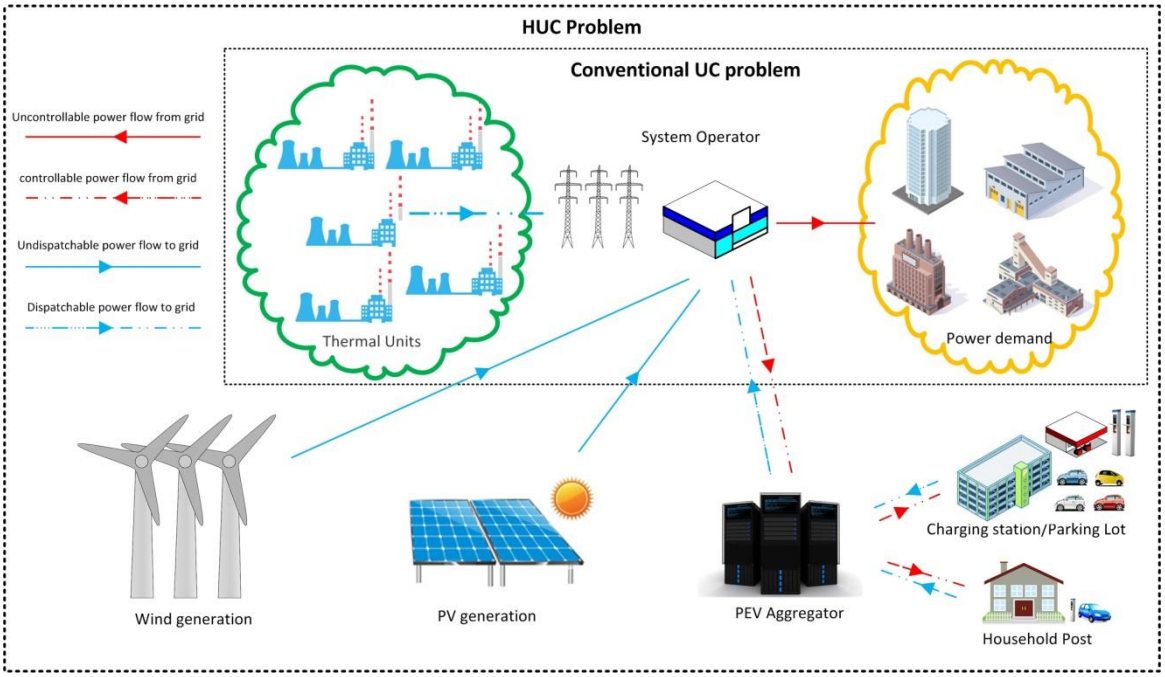

Figure 1. HUC problem structure

The aims of HUC is to minimise the economic cost by determining the on/off status of each thermal generation unit, the charging/discharging power to/from the PEVs as well as the expected generated power to be generated by each unit with 'on' status. Meanwhile, the generation limit, power demand limit, spinning reserve limit, minimum up/down limit and some other system constraints have to be met.

2.1 Objective function

The economic cost of a generation unit is composed of two parts, namely a quadratic formulation representing the fuel cost with binary unit status, and a piece-wise formulation referring to the start-up cost.

2.1.1 Fuel cost

The fuel cost function defined below is a widely adopted quadratic formulation determining the fossil fuel economic cost [10,13],

$$F_{j,t}\left(P_{j,t}\right) = a_j + b_j P_{j,t} + c_j P_{j,t}^2 \tag{1}$$

where $P_{j,t}$ and $F_{j,t}$ denote the determined power and fuel cost of the j^{th} unit in the t time interval. a_j, b_j and c_j are the fuel cost coefficients of the corresponding unit.

2.1.2 Start-up cost

Once a unit is de-committed (shut down), it needs to be reheated for restarting. The start-up cost $SU_{j,t}$ includes the cold start cost $SU_{C,j}$ which is usually higher if the de-committed period of a unit is over the cold-start hour $T_{cold,j}$ and the hot-start cost $SU_{H,j}$ which is usually lower if the de-committed period of a unit does not exceed the $T_{cold,j}$. The explicit expression is given below,

$$SU_{j,t} = \begin{cases} SU_{H,j}, if\ MDT_j \le TOFF_{j,t} \le MDT_j + T_{cold,j} \\ SU_{C,j}, if\ TOFF_{j,t} > MDT_j + T_{cold,j} \end{cases} \quad (2)$$

where MDT_j and MUT_j denote the minimum down time and minimum up time for an off/on unit to re-commit (turn on) /de-commit. The duration of the off-line status for the j^{th} unit is denoted as $TOFF_{j,t}$.

The final objective function C_{Total} is composed of the two parts defined above, associated with the binary variables $u_{j,t}$ to denote the on/off status for the j^{th} unit in the specific time slot, and it accumulates the total cost of N units in T time periods as shown below,

$$min\ C_{Total} = \sum_{t=1}^{T} \sum_{j=1}^{N} \left[F_j(P_{j,t}) u_{j,t} + SU_{j,t}(1 - u_{j,t-1}) u_{j,t} \right] \quad (3)$$

It should be noted that the start-up cost is related to the current on-line or off-line unit status and the status in previous time slot. The operational costs of wind and solar, power released from PEVs, and the battery degradation cost are not considered in this paper, and could be considered in the future work.

2.2 Constraints

In addition, several system constraints due to physical nature and power system mechanism should be considered, including generation limits of thermal power, REG and V2G power, power demand limit, spinning reserve limit, minimum up/down limit and PEV charging limit. It should be noted that some constraints such as the ramping rate and valve point effect in the economic dispatch step [50] are not considered in this paper.

2.2.1 Thermal generation limit

Each of the thermal generation units is limited by the minimum and maximum power output. The generation power needs to be dispatched within this range:

$$u_{j,t} P_{j,min} \le P_{j,t} \le u_{j,t} P_{j,max} \quad (4)$$

where $P_{j,min}$, $P_{j,max}$ represent the minimum and maximum power limit respectively.

2.2.2 *Power balance constraints*

Power demand in the HUC model is a predicted load that requires meeting by thermal unit generations. In other words, the total generated power of all online units should balance the system load demand. The HUC model considers both the thermal generation units and renewable energy sources including wind power, solar power and day-ahead PEV power dispatch. The power demand balance equation is denoted as follows;

$$\sum_{j=1}^{n} P_{j,t} u_{j,t} + P_{Wind,t} + P_{Solar,t} = P_{D,t} + P_{PEV,t} \quad (5)$$

where $P_{Wind,t}$ and $P_{Solar,t}$ are predicted wind power and solar power respectively, and $P_{D,t}$ is the predicted power demand at time t. The V2G and G2V power are generally represented as $P_{PEV,t}$ where a positive value denotes the PEV aggregator is on the G2V mode, receiving energy from grid at time t. A negative value of $P_{PEV,t}$ represents the V2G mode through which PEVs batteries deliver power back.

2.2.3 *Spinning reserve*

The power demand is a predicted value. The spinning reserve limit is designed to reserve enough power output ability to timely compensate the deviation between power supply and user demand to guarantee the safety and flexibility of the grid,

$$\sum_{j=1}^{n} P_{j,max} u_{j,t} + P_{Wind,t} + P_{Solar,t} \geq P_{D,t} + P_{PEV,t} + SR_t \quad (6)$$

As in the equation (6), SR_t is the spinning reserve at time t. The generation capacity is calculated as the sum of the maximum power output of on-line thermal units and the predicted REG.

2.2.4 *Minimum up/down time constraints*

Thermal units need to be heated up after de-committed and cooled down when over-committed, due to which it endures a minimum up or down time. As denoted in (7), if the on-line duration of a unit $TON_{j,t-1}$ is less than the minimum up time, the unit status $u_{j,t}$ needs to be forcedly turned on, and vice versa.

$$u_{j,t} = \begin{cases} 1, & if\ 1 \leq TON_{j,t-1} < MUT_j \\ 0, & if 1 \leq TOFF_{j,t-1} < MDT_j \\ 0\ or\ 1, & otherwise \end{cases} \quad (7)$$

2.2.5 *Renewable generation limit*

Wind and solar power sources are integrated in the power system under certain capacities according to the system planning. The maximum power generation of both wind and solar power are limited by their capacities due to the mechanical torque boundary for wind and chemical saturation of photovoltaic material for solar radius. The limits are shown in (8) and (9) as below,

$$P_{Wind,t} \leq P_{Wind,max} \tag{8}$$

$$P_{Solar,t} \leq P_{Solar,max} \tag{9}$$

Note that as the wind and solar power is not dispatchable, typical scenarios are considered and analysed in system scheduling [14,51]. In this paper, deterministic scenarios are considered, $P_{wind,max}$ and $P_{Solar,max}$ are the maximum generation of wind and solar power.

2.2.6 PEVs charging/discharging power limit

Load shaping demand side management (e.g. intelligent scheduling) of PEVs flexibly determines the V2G/G2V mode and determine the exact power feeding back to or receiving from the grid for PEV batteries. Due to the number and capacity of PEV chargers (for G2V use) and feeders (for V2G use), the maximum power $P_{PEV,max}$ and minimum power $P_{PEV,min}$ for PEVs are denoted in (10) as follows,

$$P_{PEV,min} \leq P_{PEV,t} \leq P_{PEV,max} \tag{10}$$

where $P_{PEV,max}$ represents the maximal charging power (positive) in the G2V mode at time t and $P_{PEV,min}$ denotes the maximal discharging power of PEVs (negative)in the V2G mode.

2.2.7 PEVs power demand limit

Another PEVs power limit is the PEV power demand limit. A certain amount of power necessity is expected for commuter PEVs to fulfil their daily transportation utilisation. This expected power for PEVs is denoted as P_{exp} in (11) which is the sum of PEV charging power from the grid.

$$\sum_{t=1}^{T} P_{PEV,t} = P_{exp} \tag{11}$$

All of these limits should be handled in the optimisation procedure, which is explicitly addressed in section 4.

3. Preliminaries of proposed algorithm

The new formulation of HUC problem reveals that it is a complex nonlinear mixed integer problem, calling for a novel powerful tool to seek a solution which is composed of integer variables determining the on/off status of each thermal unit, real valued variables for power output of online thermal units as well as real valued variables for PEV power delivery. A parallel-series hybrid meta-heuristic based optimisation is proposed which integrates a HTBPSO method to determine binary on/off status of units, a SaDE method to schedule the real valued power delivery of PEVs and the Lambda iteration method for economic load dispatch (ELD). The proposed PSH method takes the advantages of the high efficiency of the heuristic methods (e.g. the binary PSO and the SaDE) in seeking solutions for high-dimensional strong constrained binary and continuous problems, as well as the strong converging ability of lambda iteration method. Working in parallel and then series, the three approaches work co-ordinately to achieve competitive solutions for the proposed HUC problem.

3.1 Hybrid topology BPSO for binary optimisation

3.1.1 Hybrid topology binary PSO

Binary particle swarm optimisation (BPSO) is a popular discrete intelligent methods proposed in [52]. It has been utilised for solving the UC problem in [53] but endures slow convergence speed and easy to be trapped in local minimum. Multiple variants of BPSO are proposed to improve the performance by changing the probability function [54, 55, 56], to modify the evolutionary logic [57, 58, 59, 60] and to integrate within quantum-inspired computation [13, 61]. Beheshti *et al.* [56] proposed a new hybrid topology binary PSO (HTBPSO) for solving discrete optimisation problems. This method integrates the state-of-the-art techniques of both binary and continuous PSO including a modified design of the sigmoid function for speeding up algorithm convergence, a hybrid learning structure for sharing experience from global/local/neighbour best particles, introduction of an Gaussian error function as a small disturbance to improve the exploitation ability, as well as a new acceleration term to enhance the exploration ability. The procedure of HTBPSO shares similar variables and parameters definition and the velocity update section as follows;

$$v_i(t+1) = w(t) \times v_i(t) + C_1(t) \times rand_1 \times \left(p_{lbest,i} - u_i(t)\right) + C_2(t) \times rand_2 \times \left(p_{nbest,i} - u_i(t)\right) \quad (17)$$

The difference of the HTBPSO compared with the original BPSO is that the global learning term has been replaced by a neighbour learning term, where a local best particle from a neighbour position $p_{nbesti}\ (t)$ is selected to improve the learning of the current variable $u_i(t)$. This neighbour is a randomly selected one from

the whole population. The original social coefficient $C_2(t)$ has a new role defined as the counterpart coefficient to scale the neighbour learning step. This new term is designed to activate the internal information exchange of the population in order to avoid the particles being trapped in the local optimum. However, the replacement of the global learning may sacrifice the exploration ability and hinder the global convergence.

To compensate the lack of social learning term and increase the convergence speed, an acceleration is designed with the social learning associated with the velocity updating as follows,

$$a_i(t+1) = v_i(t+1) + C_3(t) \times rand_3 \times \left(p_{gbest} - u_i(t)\right) \tag{18}$$

where $a_i(t+1)$ is an acceleration. It is formulated by the sum of the updated velocity from previous two learning term and another term with the social coefficient $C_3(t)$. The vector typology of the acceleration update process is illustrated in Figure 2 below,

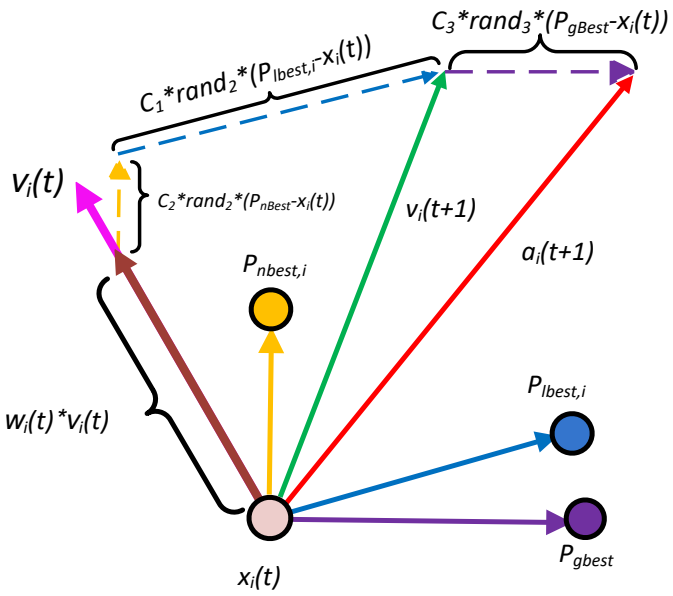

Figure 2. Hybrid typology for population update

By adding a new acceleration, the probability function of each position $P(a)$ is given as follows,

$$P(a) = |tanh(a)| \tag{19}$$

where the original sigmoid curve is modified as a symmetrical curve shown in figure 3. The large value of acceleration represents high possibility to change from the current position while the zero value means that the current value has approached the optimum and will stay at current position. The boundaries of

acceleration are limited as [-6, 6] due to that the value of probability function of this boundary has cover over 99.99% of all the possibility.

In addition to determining the final generation probability from the acceleration, a small perturbation is introduced to increase the chance for the population to jump out of the local optimums. The disturbance employed the Gaussian error function as follows,

$$E = \mathrm{erf}\left(\frac{NF}{T'}\right) = \frac{2}{\sqrt{\pi}}\int_0^{\frac{NF}{T'}} e^{-t^2}\, dt, \tag{20}$$

where *NF* is the iteration number with the best position remaining unchanged in the iteration, associated with a time constant *T'*. This Gaussian error function value *E* is embedded into the population function denoted as:

$$P\big(a_i(t+1)\big) = E + (1-E) \times \left|tanh\big(a(t+1)\big)\right| \tag{21}$$

The position is then updated by comparing the probability *P(a)* with a random number $rand_4$ with the range of (0,1) shown as:

$$u_i(t+1) = \begin{cases} 1 - u_i\,(t), & if\ rand_4 < P(a_i\,(t+1)) \\ u_i(t), & otherwise \end{cases} \tag{22}$$

As shown in (22), the new variables probability is calculated by the latest accelerations and compare with $rand_4$, and if $rand_4 < P(a_i(t+1))$, the binary variable $u_i\,(t+1)$ will change to the opposite position of $u_i(t)$.

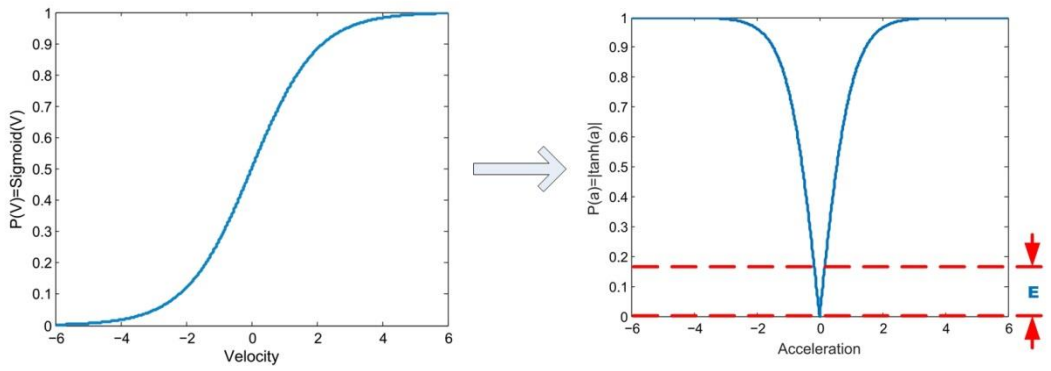

Figure 3. Probability distribution of HTBPSO

This integration of complementary perturbation strategy with previously introduced symmetric acceleration and neighbour learning strategy greatly enhance both the exploration and exploitation capability. The proposed HTBPSO will not only speed up the convergence, but also avoid solutions being trapped within local optimum.

3.2 SaDE method for real-valued optimisation problem

In parallel with the binary method, a real valued optimisation method is required to simultaneously determine the PEVs power $P_{PEV,t}$ in order to handle the system constraints (5) and (6). The DE algorithm is one of a popular meta-heuristic due to the high efficiency and simple implementation. A number of DE variants have been proposed to solve continuous constrained and unconstrained problems such as jDE [62], NSDE [63], SaDE [64], JADE [65], DEGL [66] and so on. Among these variants, SaDE has a simple structure and less parameters to tune, and therefore is used in this paper to schedule real valued $P_{PEV,t}$. Detailed process including mutation, crossover and selection operations of SaDE is illustrated as follows:

$$MV_{i,G} = \begin{cases} X_{r1,G} + F \cdot \left(X_{r2,G} - X_{r3,G}\right), & if \;\; p_s < p_1 \\ X_{i,G} + F \cdot \left(X_{best,G} - X_{i,G}\right) + F \cdot \left(X_{r1,G} - X_{r2,G}\right), & otherwise \end{cases} \tag{23}$$

where $X_{r1,G}$, $X_{r2,G}$ and $X_{r3,G}$ are three randomly selected particles in the optimisation population at G^{th} iteration and F is the mutation factor. $MV_{i,G}$, $X_{i,G}$ and $X_{best,G}$ are the i^{th} mutant vector, i^{th} particle in the population as well as best particle at G^{th} iteration. Two basic DE mutation strategies namely rand/1/bin and current to best/2/bin are selected in (23) according to the probability p_1 determined by (24) comparing with a random number p_s. The probability p_1 depends on ns_1, ns_2, nf_1 and nf_2 which denote the success and failure times of corresponding two strategies in (23).

$$p_1 = \frac{ns_1 \cdot (ns_2 + nf_2)}{ns_2 \cdot (ns_1 + nf_1) + ns_1 \cdot (ns_2 + nf_2)} \tag{24}$$

The crossover operation is denoted in (26) where CR is the crossover rate. $mv_{j,i,G}$, $x_{j,i,G}$ and $tav_{j,i,G}$ represent mutant vector, trial vector and target vector respectively.

$$tav_{j,i,G} = \begin{cases} mv_{j,i,G}, & if \;\; rand_4 < CR \; or \; j = j_{rand} \\ x_{j,i,G}, & otherwise \end{cases}, \quad j = 1,2,\dots,n \tag{25}$$

The trial vector is evaluated by the cost function f and updates the trail particle $X_{i,G+1}$ as show below.

$$X_{i,G+1} = \begin{cases} TAV_{i,G}, & if \;\; f\left(TAV_{i,G}\right) < f\left(TV_{i,G}\right) \\ X_{i,G} & otherwise \end{cases} \tag{26}$$

The SaDE algorithm is a trade-off between the exploration capability and the exploitation capability by selecting two mutation strategies and therefore can be integrated with the previously introduced binary optimisation method to effectively solve the HUC problem in a parallel-series topology.

3.3 Two Priority lists for solving the HUC problem

The priority list of the original UC problem is established as the reference in determining the order of unit commitments. However in the new HUC problem, two priority lists are produced for both the unit commitment and the charging/discharging allocation of PEVs respectively.

The original UC priority list in this paper is created by formulating an index π_j, which represents the average cost of full power generation of each unit *j* [71] and is calculated as in (27),

$$\pi_j = \frac{a_j}{P_{j,max}} + b_j + c_j \cdot P_{j,max} \tag{27}$$

By ranking the index π_j in the ascending order, the units are committed sequentially from cheapest base load units to expensive peak load units in handling the constraints (6).

Intelligent allocation of PEVs charging and discharging can shave the peak load and fill the load valley to reduce the start-up cost and expensive fuel cost from peak units. Therefore, in addition to the widely used UC index π_j, a new index δ_t is created, linking the power demand with the allocation of PEVs charging and discharging as shown below,

$$\delta_t = P_{D,t} - P_{Wind,t} - P_{Solar,t} \tag{28}$$

where the renewable generation $P_{Wind,t}$ and $P_{Solar,t}$ are taken as negative loads and removed from the original load $P_{D,t}$. The index δ_t is in ascending order for the charging allocation to schedule more PEVs load on off-peak time to preferentially fill in the load valley. Meanwhile, a descending order of index δ_t is adopted for scheduling the discharging power, providing V2G service during the peak time. Such priority list of PEVs is utilised in handling the PEVs constraint (10) and (11) and the unit scheduled priority list sequence is denoted as Δ discussed in the constraint handling subsections 4.2.

3.4 Proposed parallel-series hybrid method

The proposed PSH methods have three key components, including two parallel running algorithm blocks and a series running algorithm block. The structure of PSH is proposed as figure 4, where Block A and B are connected in parallel and Block C is linked in series with the others. Particularly, Block A is the binary algorithm which determines the on/offline status of the thermal generators in a 24 hours horizon, and HTBPSO method will be adopted in this block. Moreover, Block B runs parallelly to determine the LSDSM of PEVs in each hour of a single day, and the continuous SaDE method is employed. To achieve the dispatching results for HUC

problem, both Block A and B are connected with Block C where the lambda iteration method is utilised. The detailed implementation of the PSH method will be further addressed in Section 4.

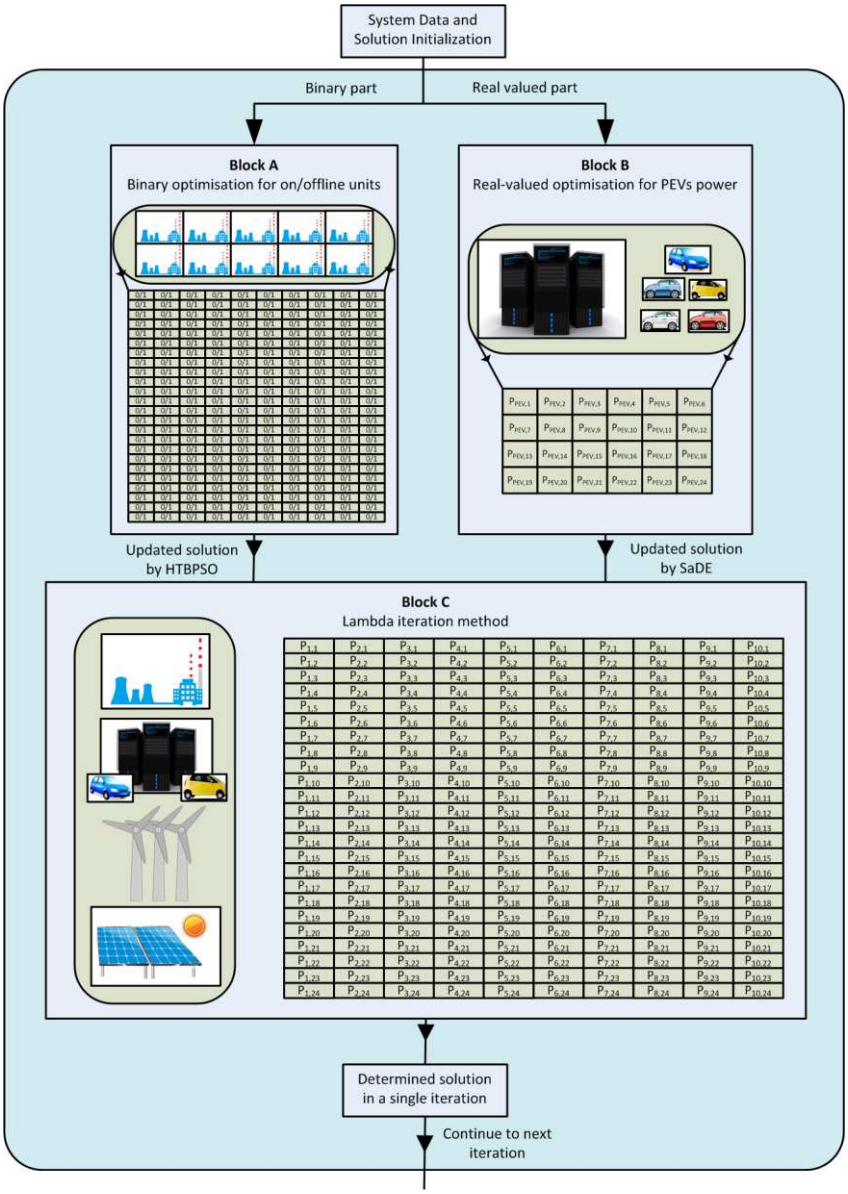

Figure 4. Proposed PSH algorithm structure

4. Implementation of the proposed parallel-series hybrid method for the HUC problems

The proposed two meta-heuristic methods are running in parallel first during the evolutionary process, one is for optimising the binary on/off-line status of units, and the other is for optimising the real-valued PEV power variables respectively, and the results are then merged during the lambda iteration for economic dispatch to optimise the real valued power generation for each online unit. The population structure in the evolutionary

process is shown in figure 5, while the proposed hybrid algorithm structure is shown in figure 6. Several key procedures are detailed in this subsection followed by the specific steps of the algorithm implementation.

4.1 Variables coding

In the proposed algorithm, three types of variables need to be optimised, including the binary on/offline variables U_i, charging/discharging power of PEVs $P_{PEV,i}$, and dispatched power of online units P shown as below,

$$U_i = \begin{pmatrix} u_{i,1,1} & u_{i,1,2} & \dots & u_{i,1,T} \\ u_{i,2,1} & u_{i,2,2} & \dots & u_{i,2,T} \\ \vdots & \vdots & \vdots & \vdots \\ u_{i,N,1} & u_{i,N,2} & \dots & u_{i,N,T} \end{pmatrix} \quad i = 1,2,\dots,Np \tag{29}$$

$$P_{PEV,i} = (p_{PEV,i,1} \quad P_{PEV,i,2} \quad \dots \quad P_{PEV,i,T}) \quad i = 1,2,\dots,Np \tag{30}$$

$$P = \begin{pmatrix} P_{1,1} & P_{1,2} & \dots & P_{1,T} \\ P_{2,1} & P_{2,2} & \dots & P_{2,T} \\ \vdots & \vdots & \vdots & \vdots \\ P_{N,1} & P_{N,2} & \dots & P_{N,T} \end{pmatrix} \tag{31}$$

where Np is the number of particles in a population of the proposed method. The dimension of the variables U_i and P_i are $N*T$ and that of $P_{PEV,I}$ is $1*T$. In the proposed PSH method, the binary population U_i and real value population $P_{PEV,i}$ are updated by HTBPSO and SaDE respectively. The variable P is calculated by the lambda iteration. The structure of a population maintained by the proposed PSH algorithm is shown as in Figure 5.

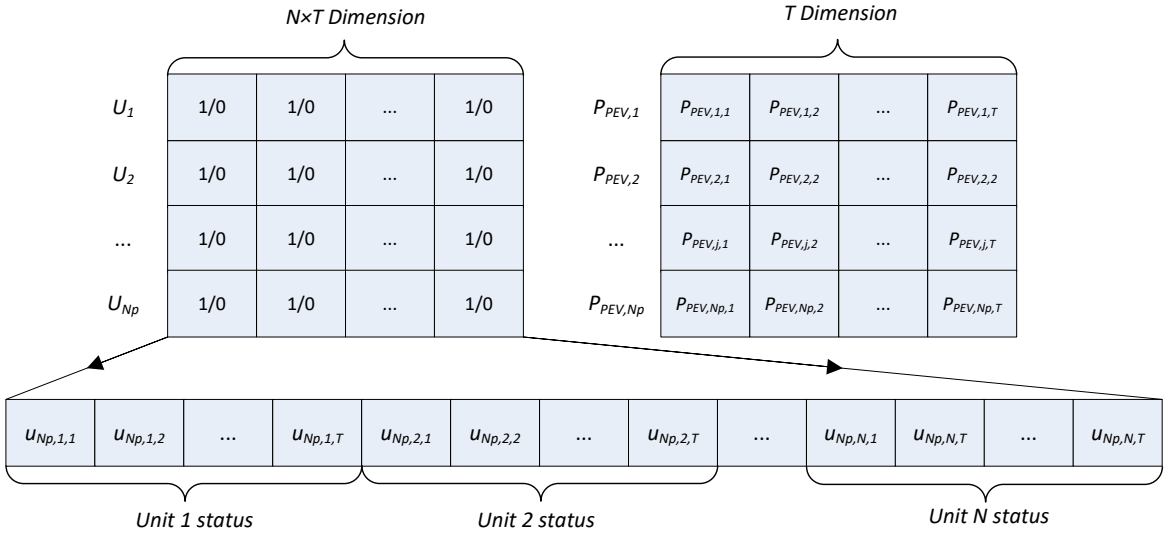

Figure 5. Structure of a population for the proposed PSH algorithm

4.2 Handling of constraints

The proposed HUC problem consists of several important system constraints that need to be handled, including the power demand limit, spinning reserve limit, minimum up/down time limit as well as PEVs power demand limit. The rule-based heuristic handling method [13] is utilised to handle the minimum up/down time and the spinning reserve limits. The detailed handling method is proposed as follows.

4.2.1 Handling of minimum up/down time limit

The minimum up/down time limit as in (7) directly affect the on/off-line status of the binary variables, and thus other constraints to be handled. Therefore, it is handled first to ensure the binary solutions are valid. The heuristic based handling method is illustrated by the pseudo-code shown below,

Begin
For j=1 to N
If $u_{j,t}$=1
If $u_{j,t-1}$=1
If $TOFF_{j,t-1}$<MDT_j
$u_{j,t}$=0;
Endif
Endif
Else
If $u_{j,t-1}$=1
If $TON_{j,t-1}$<MUT_j
$u_{j,t}$=0;
Endif
Endif
Endif
Endfor
end

4.2.2 Spinning reserve limit handling

Spinning reserve provides additional fast responsive power capacity to compensate unpredicted load demand. The detailed handling method is shown in the pseudo-code below:

Begin
Sort the generators in the ascending order of the priority list π_j
Set the generator sequence g=1
If $u_{g,t}$=0
While ($\sum_{j=1}^{n} P_{j,max} u_{j,t} + P_{Wind,t} + P_{Solar,t} \geq P_{D,t} + P_{PEV,t} + SR_t$)
If $u_{g,t}$=0
$u_{g,t}$=1
If $TOFF_{g,t}$>MDT_g
$TOFF_{g,t}$=0

$TON_{g,t}$= $TON_{g,t-1}$+1
Else
l=t-$TOFF_{g,t}$+1
While (l>t)
$u_{g,l}$=1
$TOFF_{g,t}$=0
$TON_{g,l}$= $TON_{g,l-1}$+1
l=l+1
Endwhile
Endif
Endif
g=g+1
Endwhile
Endif
End

4.2.3 De-commitment for redundant units

The above introduced handling methods for the minimum up/down time and spinning reserve limit very likely introduce redundant on-line units and lead to unnecessary cost. A de-commitment technique is employed here to tackle this issue. The specific procedure is demonstrated below:

Begin
Sort the generators in the descending order of the priority list π_j
Set the generator sequence g=1
If $u_{g,t}$=1
While ($\sum_{j=1}^{n} P_{j,max} u_{j,t} - P_{g,max} + P_{Wind,t} + P_{Solar,t} \geq P_{D,t} + P_{PEV,t} + SR_t$)
If $TON_{g,t}$>MUT_g
$u_{g,t}$=0
$TON_{g,t}$=0;
$TOFF_{g,t}$= $TOFF_{g,t-1}$+1
Elseif $TON_{g,t}$=1
$u_{g,t}$=0
$TON_{g,t}$=0
$TOFF_{g,t}$= $TOFF_{g,t-1}$+1
Endif
g=g+1
Endwhile
Endif
End

4.2.4 Handling of PEVs limits

The PEVs charging/discharging limit (10) is the total power of PEVs that needs to be charged or the minimum power capacity of PEVs that can provide V2G service. The power demand limit (11) is the total power needed from the grid to the aggregator of PEVs for supporting the daily demand. We propose a load levelling based

method to handle these limits. The power mismatch P_{De} is handled according to the PEV scheduling priority list δ_t defined in Subsection 3.3. The detailed procedure is given below.

Begin
Sort load demand according to the ascending order of the priority list δ_t in the sequence Δ
For t=1 to T
If $P_{PEV,t}<P_{PEV,t,min}$
$P_{PEV,t} = P_{PEV,t,min} + rand \cdot (P_{PEV,t,max} - P_{PEV,t,min})$
Elseif $P_{PEV,t}>P_{PEV,t,max}$
$P_{PEV,t} = P_{PEV,t,min} + rand \cdot (P_{PEV,t,max} - P_{PEV,t,min})$
Endif
$P_{De} = P_{Exp} - \sum_{j=1}^{n} P_{PEV,t}$
If $P_{De}>0$
while ($P_{De}>0$)
j=j+1
$P_{De,Tem} = P_{PEV,t,max} - P_{PEV,\Delta(j)}$
If $P_{De}> P_{De,Tem}$
$P_{PEV,\Delta(j)} = P_{PEV,t,max}$
$P_{De} = P_{De} - P_{De,Tem}$
Else
$P_{PEV,\Delta(j)} = P_{PEV,\Delta(j)} + P_{De}$
Endif
Endwhile
Elseif $P_{De}<0$
while ($P_{De}<0$)
j=j+1
$P_{De,Tem} = P_{PEV,t,min} - P_{PEV,\Delta(T-j+1)}$
If $P_{De}< P_{De,Tem}$
$P_{PEV,\Delta(T-j+1)} = P_{PEV,t,min}$
$P_{De} = P_{De} - P_{De,Tem}$
Else
$P_{PEV,\Delta(T-j+1)} = P_{PEV,\Delta(T-j+1)} + P_{De}$
Endif
Endwhile
Endif
Endfor
End

In the procedure, $P_{De,Tem}$ denotes the temporary power deviation between the limit and the scheduled PEVs power in the priority list sequence Δ, which denoted as $P_{PEV,\Delta(j)}$ or $P_{PEV,\Delta(T-j+1)}$. In this method, the unsatisfied power is met at the off-peak time and the excessive power is released at the peak time. In addition, the intelligent load levelling method also limits the scheduled PEVs power within the charging/discharging boundary.

4.3 Lambda iteration based ELD

Lambda iteration method is a popular technique to solve constrained non-linear optimisation problems. It has been widely employed in solving economic load dispatch problem [12,14,22,71]. The power demand limit and generation limit is relaxed and handled during the iteration procedure. The specific pseudo-code of the lambda iteration method is given below.

Begin

Given by an alternative solution $U_{i,t}=\{u_{i,1,t}, u_{i,2,t},\ldots, u_{i,N,t}\}$, $P_{D,t}$ and system parameters;
Set permitted error ξ_0=0.1, maximum iteration $Iter_{Max}$=200;
Set initial value λ_k;
While ($|\xi_k| \geq \xi_0$) do
Calculate $P_j' = \frac{\lambda_t - b}{2c}$
Calculate $P_{j,t} = min\{max\{P_j', P_{j,min}\}, P_{j,max}\}$;
Calculate $\xi_k = \sum_{j=1}^{n} P_{j,t} \cdot u_{j,t} - P_{D,t} - P_{PEV,t} + P_{Wind,t} + P_{Solar,t}$;
If ($\xi < 0$) then
$\lambda_k = \lambda_k - \Xi_k$
Else
$\lambda_k = \lambda_k + \Xi_k$
Endif
calculate $\Xi_{k+1} = \Xi_k + \frac{\Delta_k - \Delta_{k-1}}{\xi_k - \xi_k - 1} \cdot (P_{D,t} + P_{PEV,t} - P_{Wind,t} - P_{Solar,t})$;
k=k+1;
Endwhile

End

The acceptable duality gap ξ_0 is set as 0.1 and the feasible λ_k is updated by an inertial parameter Ξ_k, which is dynamically determined at every iteration.

4.4 Implementation of the proposed PSH method

By employing the above constraints handling method, the algorithm structure can now be given in Figure 6. A deterministic scenario is adopted in this paper for algorithm performance tests.

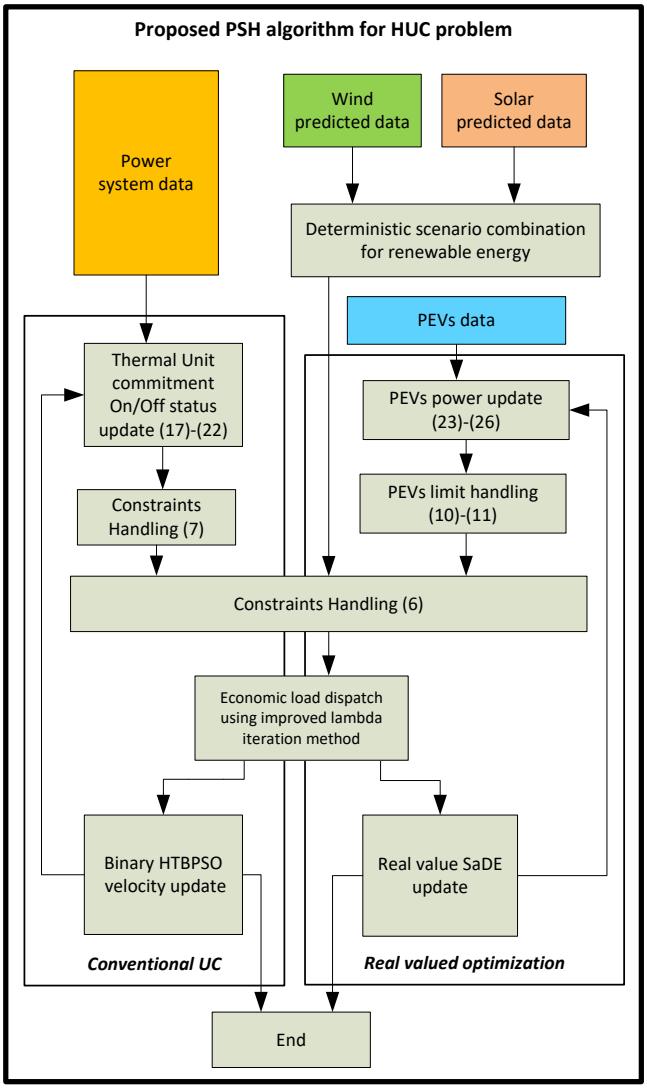

Figure 6. Structure of the implementation for the proposed PSH algorithm

The implementation process is summarised in the following steps:

Step 1. Generation of scenario for renewable energy

a) Import predicted wind and solar power generations for a given period ;

b) Generate a deterministic combined scenario of renewable energy as the input of HUC problem;

Step 2. Initialisation

a) Import the power system data and parameters including generation capacity, minimum up/down time, fuel coefficients, start-up and shut-down cost of the units and predicted load demand etc.;

b) Import the PEVs data including charging and discharging capacity and power demand;

c) Import the renewable generation scenario.

d) Initialise HTBPSO algorithm parameters such as C_1, C_2, C_3, w, iteration and particle numbers;

e) Initialise SaDE algorithm parameters such as F, CR, iteration and particle numbers;

f) Randomly generate populations for both algorithms, handling all the constraints using methods in 4.2;

g) Compute the objective function for each U_i in the binary population and real-valued $P_{PEV,i}$ using Lambda iteration method to determine the local best and global best particles from the initial population;

Step 3. Hybrid parallel-series process for HUC

a) Update the velocity according to (17) and (18), update the probability amplitude based on (20)-(21), generate a new binary population according to (22) and repair the minimum up/down time limit as detailed in 4.2.1;

b) Update real-valued variable according to (23)-(25) and repairs the PEV power limit as detailed in 4.2.4;

c) Repair all the new particles U_i associated with renewable generation scenarios and PEVs variables to avoid violating spinning reserve limit and over committing, as detailed in 4.2.2 and 4.2.3;

d) Compute the objective function for each U_i and $P_{PEV,i}$ in the population using Lambda iteration method as detailed in 4.3, update the local best and global best particles of HTBPSO and implement selection operation of SaDE as in (26);

e) If the iteration is less than $iter_{max}$, go back to Step 3-a, otherwise, go to the Step 4.

Step 4. Performance evaluation

a) Record the optimisation result, go back to Step 2.

b) The economic cost of the scenarios are compared and analysed.

It should be noted that the Step 3-a and 3-b illustrate the parallel Block A and Block B in Figure 4, whereas the Step 3-d elaborates the series Block C in the same figure. The Using the proposed PSH method, various scenarios of REG and LSDSM of PEVs in the conventional UC problem could be evaluated and compared in terms of the economic impact on the power system operation.

5. Numerical results and analysis

The new PSH method provides a powerful tool to solve both the conventional UC problems and the HUC problem considering intermittent REG and PEVs intelligent charging and discharging. In this section, the

HTBPSO, is first compared with some state-of-the-art optimisation methods on conventional UC problem in case 1. Then, the proposed PSH method is evaluated on a HUC problem considering a deterministic scenario of renewable generations and intelligent scheduling of PEVs in case 2.

5.1 Case 1: 10 Units only

In this case, the widely used 10-unit 24 hour system is employed [67], and the detailed system data is illustrated as Table 2. To fairly compare the performance of the HTBPSO with some other methods on the conventional UC problem, REG and PEVs are not considered in this case study. The optimisation is implemented in the MATLAB ®2014a on an Intel i5-3470 CPU at 3.20GHz and 8GB RAM personal computer. Thirty independent trials were run to reduce the randomness effect, where the best, mean and worst values for each run were calculated. In addition to the HTBPSO algorithm proposed in this paper, existing PSO methods including NBPSO [54] and BLPSO [56] are tested. The parameters setting for these methods are given in the Table 1 according to the original settings in [40] [41]. The number of particles in a population is 20 and the maximum iteration as 1000 as utilised in other publications [13,14,22]. The spinning reserve is 10% of predicted demand for this scenario test.

Table 1.
Parameter settings of some BPSO variants

Algorithm	Parameter settings
BLPSO	$w(t)$: 0.9-0.4, C_1=C_2=2
NBPSO	$w(t)$: 0.9-0.4, C_1=C_2=2
HTBPSO	$w(t)$: 0.6-0.2, C_1: 0.5-2.0, C_2: 1.0-2.0, C_3: 0.5-1.5, T'=500

Table 2.
10-unit benchmark system data

Parameters	U1	U2	U3	U4	U5	U6	U7	U8	U9	U10
P_{max} (MW)	455	455	130	130	162	80	85	55	55	55
P_{max} (MW)	150	150	20	20	25	20	25	10	10	10
a ($/h)	1000	970	700	680	450	370	480	660	665	670
b ($/MWh)	16.19	17.26	16.6	16.5	19.7	22.26	27.74	25.92	27.27	27.79
c ($/MWh^2)	0.00048	0.00031	0.002	0.00211	0.00398	0.00712	0.00079	0.00413	0.00222	0.00173
MUT (h)	8	8	5	5	6	3	3	1	1	1
MDT (h)	8	8	5	5	6	3	3	1	1	1
SU_H ($)	4500	5000	550	560	900	260	260	30	30	30
SU_C ($)	9000	10000	1100	1120	1800	520	520	60	60	60
T_{cold} (h)	5	5	4	4	4	2	2	0	0	0
Initial States (h)	8	8	-5	-5	-6	-3	-3	-1	-1	-1

To make a comprehensive comparison, the results by a few other state-of-the-art methods, including an efficient hybrid PSO (HPSO) [67], an improved PSO (IPSO) [68], a quantum inspired PSO (QPSO) [13], a binary real coded firefly (BRCFF) algorithm [69], a Lagrangian Relaxation and PSO method (ELRPSO) [70], a quantum inspired gravitational search algorithm (QGSA) [14], a gravitational search algorithm (GSA) [71], and an advanced three-stage approach (ATHS) [72] are listed in table 3, together with the experimental results by BLPSO, NBPSO and HTBPSO.

Table 3.
Simulation results of case 1-1 (10% spinning reserve)

Methods	Best cost ($/day)	Worst cost ($/day)	Mean cost ($/day)	SD ($/day)
HPSO [67]	563,942	565,785	564,772	—
IPSO [68]	563,954	564,579	564,162	0.11%
QPSO [13]	563,977	563,977	563,977	0
BRCFF [69]	563,937	565,597	564,743	—
ELRPSO [70]	563,938	563,977	563,971	—
BGSA [71]	563,937	564,241	564,031	114
QGSA [14]	563,937	564,390	564,065	—
ATHS [72]	563,938	564,000	563,946	19
BLPSO	563,937	564,018	563,963	22
NBPSO	563,937	563,977	563,955	20
HTBPSO	**563,937**	**563,937**	**563,937**	**0**

From the Table 3, It is clear that, HTBPSO shows the best and robust performance, achieving the best results in all 30 trials with 563,937 $/day. The results distributions of all the 30 runs by BLPSO, NBPSO and HTBPSO are further illustrated in figure 7.

Table 4.
Best unit scheduling results for Case 1-1: 10 unit-only (10% spinning reserve)

Hour	U1 (MW)	U2 (MW)	U3 (MW)	U4 (MW)	U5 (MW)	U6 (MW)	U7 (MW)	U8 (MW)	U9 (MW)	U10 (MW)	Demand (MW)	Spinning Reserve(MW)
1	455	245	0	0	0	0	0	0	0	0	700	210
2	455	295	0	0	0	0	0	0	0	0	750	160
3	455	370	0	0	25	0	0	0	0	0	850	222
4	455	455	0	0	40	0	0	0	0	0	950	122
5	455	390	0	130	25	0	0	0	0	0	1000	202
6	455	360	130	130	25	0	0	0	0	0	1100	232
7	455	410	130	130	25	0	0	0	0	0	1150	182
8	455	455	130	130	30	0	0	0	0	0	1200	132
9	455	455	130	130	85	20	25	0	0	0	1300	197
10	455	455	130	130	162	33	25	10	0	0	1400	152
11	455	455	130	130	162	73	25	10	10	0	1450	157

12	455	455	130	130	162	80	25	43	10	10	1500	162
13	455	455	130	130	162	33	25	10	0	0	1400	152
14	455	455	130	130	85	20	25	0	0	0	1300	197
15	455	455	130	130	30	0	0	0	0	0	1200	132
16	455	310	130	130	25	0	0	0	0	0	1050	282
17	455	260	130	130	25	0	0	0	0	0	1000	332
18	455	360	130	130	25	0	0	0	0	0	1100	232
19	455	455	130	130	30	0	0	0	0	0	1200	132
20	455	455	130	130	162	33	25	10	0	0	1400	152
21	455	455	130	130	85	20	25	0	0	0	1300	197
22	455	455	0	0	145	20	25	0	0	0	1100	137
23	455	455	0	0	0	20	0	0	0	0	900	90
24	455	345	0	0	0	0	0	0	0	0	800	110
Total economic cost (563,937 $/day)												

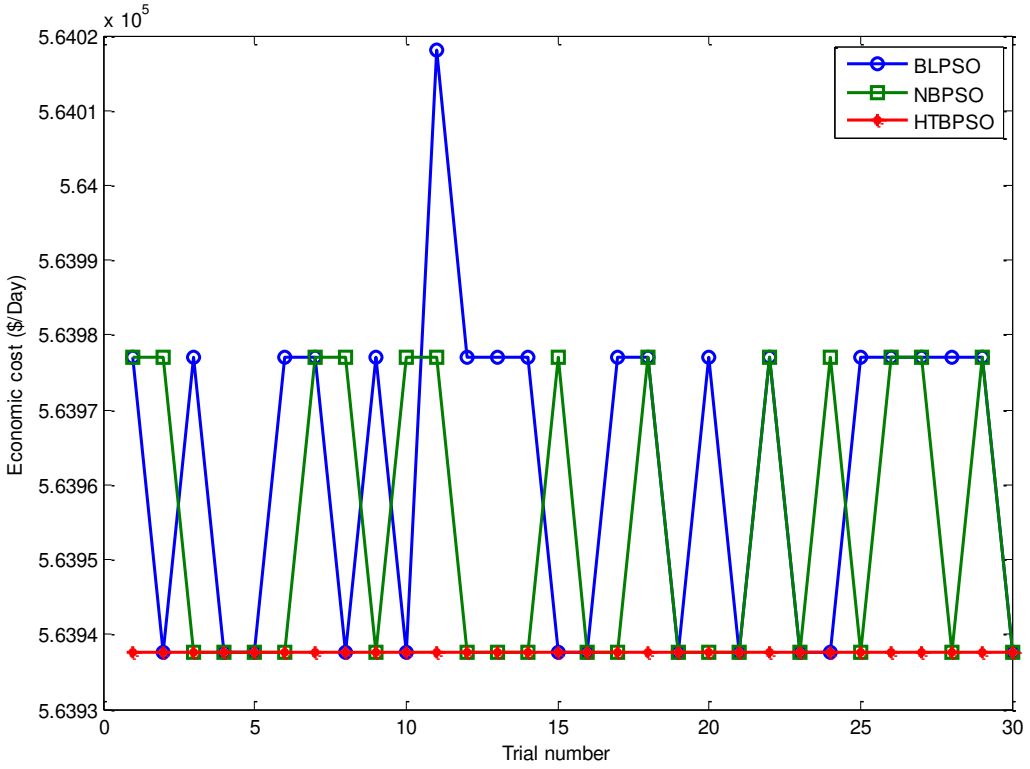

Figure 7. Result distribution of all some BPSO variants

To analyse the convergence speed of the optimisers, their average evolution processes are shown in the Figure 8.

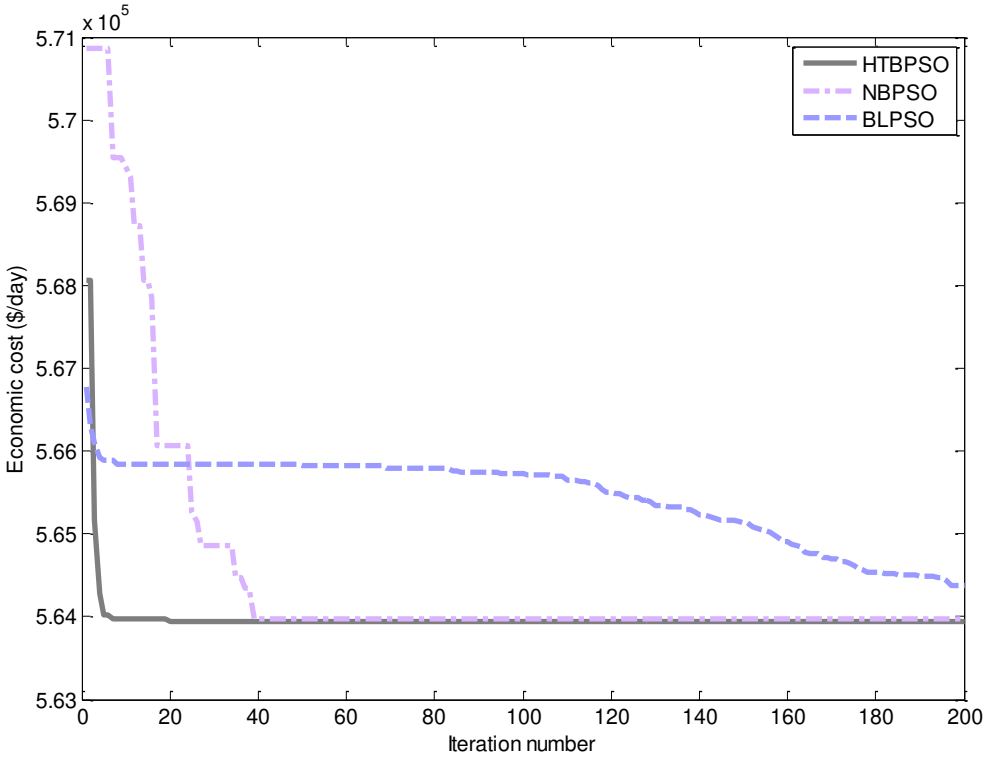

Figure 8. Average iteration process of BPSO variants

In Figure. 8, it is shown that HTBPSO converged amazingly fastest, achieving the near-optimum within only 10 iterations, followed by the NBPSO which converged to the optimum within around 40 iterations. Table 5 details the average optimising results of the 30 different runs from 20 to 1000 iterations, along with the corresponding computing time (CT).

Table 5.
Average optimising results in the iteration process

Iteration	20	CT (s)	50	CT (s)	100	CT (s)	200	CT (s)	500	CT (s)	1000	CT (s)
BLPSO	567,180	5.2	566,480	11.5	565,275	21.8	564,415	42.7	563,968	105.3	563,963	205.2
NBPSO	566,016	4.7	564,035	10.0	563,975	18.8	563,970	37.9	563,970	90.6	563,955	180.4
HTBPSO	**563,977**	4.7	**563,977**	10.1	**563,959**	18.8	**563,937**	36.2	**563,937**	88.8	**563,937**	175.7

It is clear from Table 5 that HTBPSO achieved the best result in all trials within 200 iterations, significantly outperforming BLPSO and NBPSO. The computational times for the three algorithms were almost similar and proportionally increased with the iteration numbers, and were better than other similar approaches like the QGSA with lambda iteration method [14].

To further test the performance of the proposed HTBPSO algorithm, the 10-unit system with 5% spinning reserve was evaluated. The number of particles and the maximum iterations are 20 and 200 respectively. The

traditional BPSO [53], GA [53], an adaptive PSO (APSO) [73], a binary programming (BP) [73], a two-stage based genetic algorithm (TSGB) [74], an improved IPSO [75], a three stage method B.SMP and A. SMP [76], and a hybrid harmony search (HHS) [77] are all compared in Table 6.

Table 6.
Simulation results of case 1-2 (5% Spinning reserve)

Methods	Best cost ($/day)	Worst cost ($/day)	Mean cost ($/day)
BPSO[53]	565,804	567,251	566,992
GA[53]	570,781	576,791	574,280
APSO[73]	561,586	—	—
BP[73]	565,450	—	—
TSGB[74]	560,263.92	—	—
IPSO[75]	558,114.80	—	—
B.SMP[76]	558,844.76	559,154.98	558,937.24
A.SMP[76]	557,676.81	557,987.02	557,769.28
HHS[77]	557,905.64	558,682.01	558,267.2
BLPSO	557,443.93	557,965.27	557,613.19
NBPSO	557,265.02	557,982.87	557,529.98
HTBPSO	**557,161.59**	**557,879.45**	**557,496.00**

Again, it is confirmed from Table 6 that the proposed HTBPSO achieved the lowest cost 557,161.59$/day, remarkably outperforming other counterparts in all statistics. It is clear that the new HTBPSO method outperformed state-of-the-art methods in this 10-unit commitment case. The proposed method provides a powerful tool to schedule more complicated unit commitment problems which integrate the wind power, PV generation as well as the flexible charging load of PEVs associated with SaDE method.

5.2 Case 2: 10 Units with integration of wind and solar generations and PEV charging/discharging

In this case, the HUC problem is solved by proposed PSH method where the aforementioned HTBPSO works together with SaDE to simultaneously determine the on/off status of thermal power generating units and LSDSM of PEVs power, followed by the lambda iteration method used for solving the power contributions of online units. The deterministic wind and solar power generations and aggregation of a large number of PEVs are integrated in the problem and need to be addressed all together. The spinning reserve in this case is assumed to be 10% of the accumulated power demand, which need to be provided by thermal generators. Here the PEV charging/discharging load is a positive/negative load depending on either the G2V or the V2G mode, whereas the REG generation are considered as negative loads as shown in (32).

$$SR_t = SRR \cdot (P_{D,t} + P_{PEV,t} - P_{Wind,t} - P_{Solar,t}) \quad (32)$$

where *SRR* is the spinning reserve rate as set as 10% in this case study. In the following section, the system test data and algorithm configuration are first addressed, followed by extensive simulation studies.

5.2.1 System and algorithm configuration

It is assumed that a total 50,000 PEVs are involved in discharging and 36,125 PEVs are employed in charging of LSDSM in the 10-unit commitment system with the average battery capacity of 15kWh. According to the National Household Travel Survey [78], the average daily travel distance for a vehicle is 32.88 miles. An energy necessity of 8.22kWh (0.25kWh/mile for PEVs) is therefore required to support this, and the total power necessity of PEVs is calculated as 50,000×8.22kWh=411MWh. It is also assumed that the charging and discharging efficiency of PEVs is 85% and at most 20% of total PEVs with 50% of their battery state of charge are available for charging and discharging allocation at any time [46]. The discharging power boundaries of PEVs $P_{PEV,min}$ is calculated as PEVs number 50,000 × battery capacity 15KWh × available SOC 50% × available PEVs 20% × efficiency 85% / 1h × (-1)=-63.75MW, whereas the maximum charging power $P_{PEV,max}$ is calculated as PEVs number 36,125 × battery capacity 15KWh × available SOC 50% × available PEVs 20% / efficiency 85% / 1h = +63.75MW. In addition to PEVs, a deterministic wind and solar power generation scenario is integrated in the HUC problem, using the data from [46]. The priority list index δ_t for PEVs power allocation is calculated as in (28) and ranked in an ascending order shown in Table 7. According to this index, the priority order of hours is produced as the reference for the charging/discharging allocation of PEVs LSDSM.

Table 7.
The priority list of PEV charging dispatch

Priority(Δ)	**1**	**2**	**3**	**4**	**5**	**6**	**7**	**8**	**9**	**10**	**11**	**12**
Hour	1:00	2:00	24:00	3:00	23:00	4:00	5:00	17:00	16:00	6:00	22:00	18:00
Demand (MW)	700	750	800	850	900	950	1,000	1,000	1,050	1,100	1,100	1,100
Solar (MW)	0	0	0	0	0	0	0	0	12.92	0	0	0
Wind (MW)	10.54	22.27	2.55	25.5	0	25.5	25.5	25.5	14.62	25.5	21.42	19.04
δ_t	689.46	727.73	797.45	824.5	900	924.5	974.5	974.5	1,022.46	1,074.5	1,078.58	1,080.96
Priority(Δ)	**13**	**14**	**15**	**16**	**17**	**18**	**19**	**20**	**21**	**22**	**23**	**24**
Hour	7:00	8:00	15:00	19:00	9:00	14:00	21:00	13:00	10:00	20:00	11:00	12:00
Demand (MW)	1,150	1,200	1,200	1,200	1,300	1,300	1,300	1,400	1,400	1,400	1,450	1,500

Solar (MW)	0.09	17.46	9.7	0	31.45	31.59	0	36.78	36.01	0	38.06	35.93
Wind (MW)	25.5	25.5	20.74	25.5	25.5	24.82	25.5	25.5	25.5	18.02	25.5	25.5
δ_t	1,124.41	1,157.04	1,169.56	1,174.5	1,243.05	1,243.59	1,274.5	1,337.72	1,338.49	1,381.98	1,386.44	1,438.57

In the priority list of PEVs LSDSM, the off-peak load periods 1:00, 2:00 and 24:00 rank high to have the privilege for charging power allocations, whereas the index δ_t are the largest during the peak time at 12:00, 11:00 and 20:00 which indicates that the discharging power from PEVs is preferred to offer V2G service. The solar and wind power are accumulated as negative load. The detailed priority order with the corresponding index is shown in Figure 9. By adopting this priority order, the PEVs power is consequently scheduled into the 24-hour time horizon while the PEV power constraints formulated in (10) and (11) are handled.

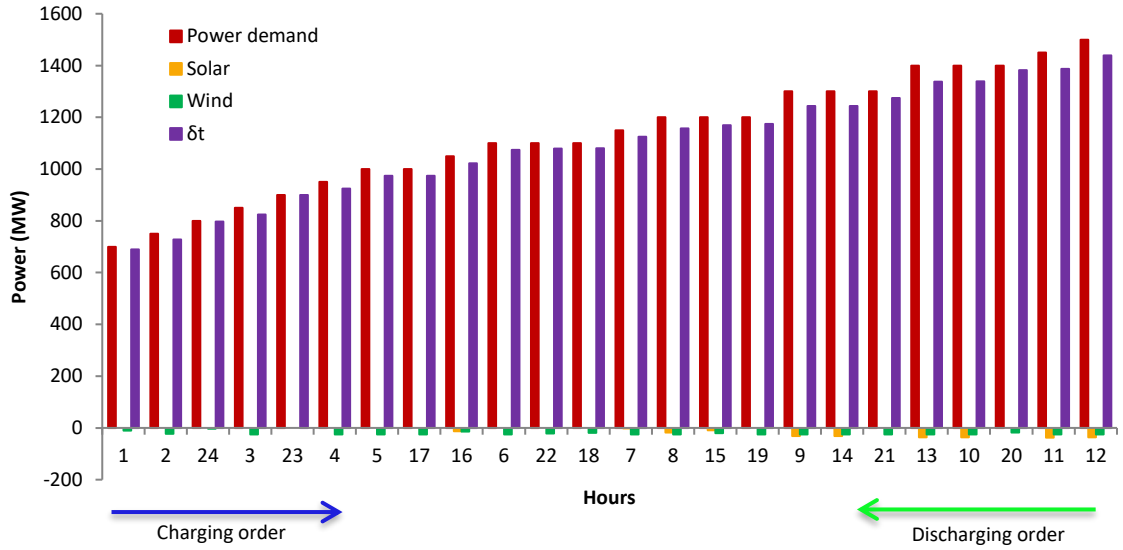

Figure 9. Priority list for charging and discharging of PEVs

Given the system data and priority lists, the proposed PSH method was then used to solve HUC problem. The parameter settings for HTBPSO given in Table 1 were adopted in this case. For the SaDE method, the mutation factor *F* and crossover rate *CR* are key parameters of the algorithm and need to be properly tuned [64]. To achieve the best configuration, a comprehensive parameter study was employed with the both parameters ranging from 0.1 to 0.9 respectively, and the results are shown in Table 8. The optimisation result for each parameter set was the best performance achieved among 10 different runs, where the number of particles in a population is 20 and the maximum iteration as 200.

Table 8.
Results achieved for SaDE parameter tuning of the proposed PSH meta-heuristic method ($/day)

Parameter settings		CR=0.1	CR=0.2	CR=0.3	CR=0.4	CR=0.5	CR=0.6	CR=0.7	CR=0.8	CR=0.9
F=0.1	Best	547,404	546,782	546,941	547,324	547,110	547,901	546,934	548,355	547,948
	Mean	548,643	548,032	548,371	548,480	548,402	548,694	547,910	548,891	548,956
F=0.2	Best	546,377	546,274	546,389	546,388	546,767	546,986	547,342	547,390	548,443
	Mean	547,134	547,361	547,164	547,576	547,639	548,004	548,398	548,432	549,098
F=0.3	Best	545,986	546,115	545,696	545,966	546,323	546,517	546,475	546,262	547,929
	Mean	546,514	546,637	546,788	546,954	547,019	547,373	547,368	547,974	548,506
F=0.4	Best	545,847	545,715	545,823	545,459	545,679	545,706	545,686	546,279	547,433
	Mean	546,088	546,408	546,114	546,153	546,372	546,412	546,830	547,692	548,360
F=0.5	Best	545,455	545,703	545,652	545,382	545,379	545,469	545,815	545,467	546,219
	Mean	545,929	546,216	546,408	545,883	546,362	546,229	546,768	547,038	547,307
F=0.6	Best	545,902	545,807	547,595	545,468	545,404	545,423	545,421	545,361	545,801
	Mean	546,111	546,246	548,136	546,034	545,879	546,231	546,345	546,501	546,601
F=0.7	Best	545,375	545,390	545,404	545,363	545,416	545,416	545,409	545,688	545,405
	Mean	545,827	546,050	546,254	545,922	546,197	546,139	546,559	546,476	546,347
F=0.8	Best	545,848	545,482	**545,294**	545,433	545,506	545,431	545,836	545,856	545,716
	Mean	545,968	546,312	545,886	546,019	545,925	546,642	546,682	546,565	546,590
F=0.9	Best	545,642	545,369	545,496	545,438	545,470	545,547	545,481	545,477	545,440
	Mean	545,780	546,049	546,100	546,131	545,923	546,354	546,252	546,798	547,059

According to Table 8, the best result was achieved for the set *F*=0.8 and *CR*=0.3 and this parameter set was adopted in the following case studies.

5.2.2 Case study 2-1, 411MW expected power for PEVs

Two scenarios with different expected power for PEVs are considered. In case study 2-1, P_{exp} from the thermal generations is set as aforementioned 411 MW to satisfy the daily commuting utilisation for users. In case study 2-2, P_{exp} from the thermal generation units is assumed to be 0 MW where PEVs are utilised as 'energy sponge' to intelligently absorb power from the grid or supply power back to the grid to fulfil the LSDSM, while the power needed to support the daily utilisation for PEVs is supposed to be provided by renewable generations, and the performance of proposed PSH algorithm is compared with the results from previous studies [44,46].

In this case study 2-1, two BPSO variants counterparts BLPSO and NBPSO and six DE variants including DE/rand/1, DE/current to best/1, DE/current to best/2, DE/best/1, DE/best/2 and DE/rand/2 were adopted [79] in the hybrid algorithm structure to compare with the proposed HTBPSO+SaDE method. Each method was tested with 10 independent runs, also the number of particles was set as 20 and the number of iterations was 200. The economic costs, the standard deviation and average computational time (CT) of these 10 independent runs are shown in Table 9, and the evolutionary process of different methods is illustrated in figure 10.

Table 9.
Numerical results for HUC considering DSLSM of PEVs (411MW) and REG

Scenarios	Cost ($/day)				CT (s)
	Best	Worst	Mean	SD	
BLPSO+SaDE	546,461	547,341	546,792	342	47.9
NBPSO+SaDE	545,867	547,221	546,281	516	48.0
HTBPSO+DE/rand/1	545,390	548,104	546,033	783	51.3
HTBPSO+DE/current to best/1	545,396	**546,336**	545,979	326	50.7
HTBPSO+DE/current to best/2	546,244	547,841	547,422	491	45.1
HTBPSO+DE/best/1	545,746	547,281	546,177	478	46.8
HTBPSO+DE/best/2	545,778	547,325	546,263	527	48.0
HTBPSO+DE/rand/2	545,802	547,646	546,501	639	45.5
PSH	**545,294**	547,278	**545,886**	652	43.7

It is clear from Table 9 that the proposed PSH method outperforms the other methods. The average computational time ranges from 43.7 to 51.3 seconds. The time difference is mainly due to the various computational efforts in handling constraints. The second best method is HTBPSO+ DE/current to best/1, achieving the smallest standard deviation 326 $/day. In terms of the convergence, it is clear from figure 10 that the HTBPSO based algorithms converged noticeably faster than other BPSO variants. The proposed PSH method achieved the best results within 200 iterations.

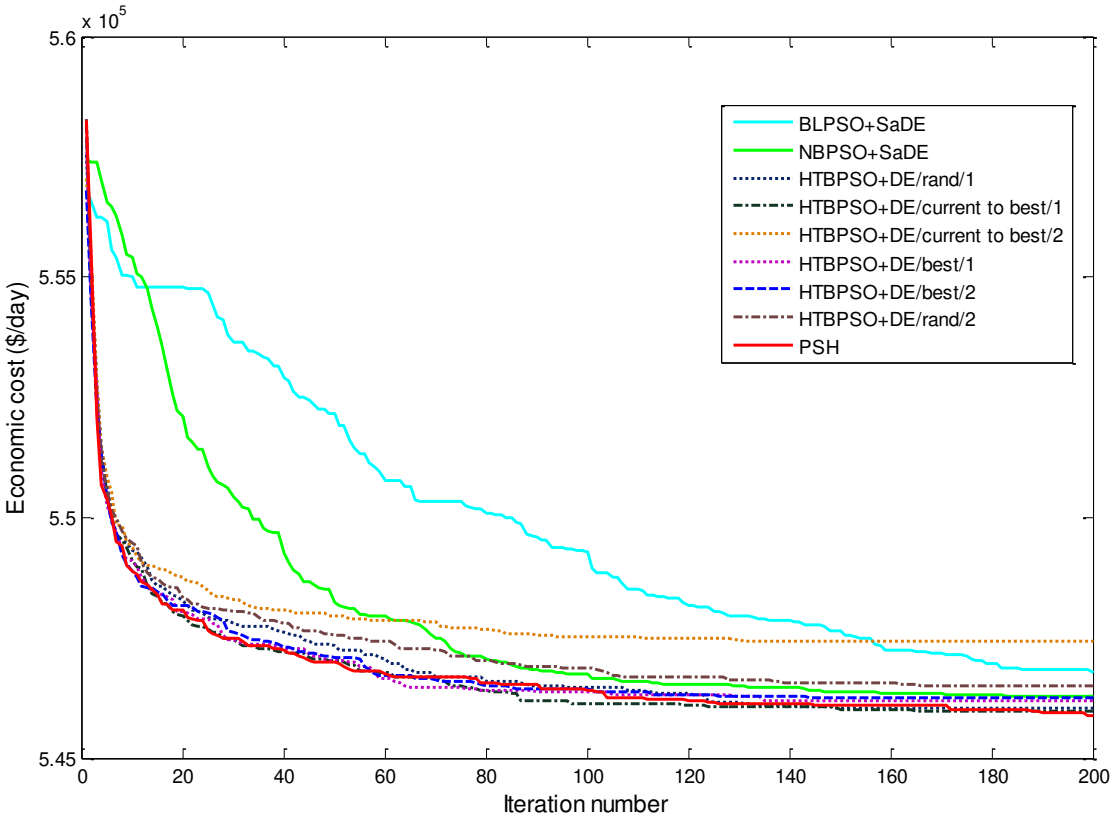

Figure 10. Average evolutionary process of variants combinations

The best scheduling plan for supplying P_{exp}=411MW is shown in Table 10. In the G2V/V2G column of the table, a positive number represents the G2V power and a negative number denotes the V2G power. The demand shown in the table is the accumulated power of positive load including predicted demand and LSDSM of PEVs, as well as negative demand of REG. The grids in green and orange denote the units that commitment was avoided, and the extra units that are committed respectively compared with the best result presented in case 1-1 shown in Table 4. The grids in pink and blue represent that the PEVs are in G2V and V2G modes respectively.

Table 10.
Best unit scheduling result of 411WM PEVs load achieved by proposed PSH method

Hour	U1 (MW)	U2 (MW)	U3 (MW)	U4 (MW)	U5 (MW)	U6 (MW)	U7 (MW)	U8 (MW)	U9 (MW)	U10 (MW)	G2V/V2G (MW)	Solar (MW)	Wind (MW)	Demand (MW)	Power reserve (MW)
1	455.00	298.21	0.00	0.00	0.00	0.00	0.00	0.00	0.00	0.00	**63.75**	0.00	10.54	753.21	156.79
2	455.00	336.48	0.00	0.00	0.00	0.00	0.00	0.00	0.00	0.00	**63.75**	0.00	22.27	791.48	118.52
3	455.00	408.25	0.00	0.00	25.00	0.00	0.00	0.00	0.00	0.00	**63.75**	0.00	25.50	888.25	183.75
4	455.00	455.00	0.00	0.00	58.91	0.00	0.00	0.00	0.00	0.00	**44.41**	0.00	25.50	968.91	103.09
5	455.00	428.25	**130.00**	**0.00**	25.00	0.00	0.00	0.00	0.00	0.00	**63.75**	0.00	25.50	1,038.25	163.75
6	455.00	398.25	130.00	130.00	25.00	0.00	0.00	0.00	0.00	0.00	**63.75**	0.00	25.50	1,138.25	193.75

7	455.00	443.03	130.00	130.00	25.00	0.00	0.00	0.00	0.00	0.00	**58.62**	0.09	25.50	1,183.03	148.97
8	455.00	455.00	130.00	130.00	32.47	0.00	0.00	0.00	0.00	0.00	**45.43**	17.46	25.50	1,202.47	129.53
9	455.00	448.46	130.00	130.00	25.00	**0.00**	**0.00**	0.00	0.00	0.00	**-54.59**	31.45	25.50	1,188.46	143.54
10	455.00	455.00	130.00	130.00	84.74	20.00	**0.00**	**0.00**	0.00	0.00	**-63.75**	36.01	25.50	1,274.74	137.26
11	455.00	455.00	130.00	130.00	122.69	20.00	**0.00**	10.00	0.00	0.00	**-63.75**	38.06	25.50	1,322.69	144.31
12	455.00	455.00	130.00	130.00	162.00	22.82	**0.00**	10.00	10.00	**0.00**	**-63.75**	35.93	25.50	1,374.82	147.18
13	455.00	455.00	130.00	130.00	83.97	20.00	**0.00**	**0.00**	0.00	0.00	**-63.75**	36.78	25.50	1,273.97	138.03
14	455.00	455.00	130.00	130.00	29.23	**0.00**	**0.00**	0.00	0.00	0.00	**-44.36**	31.59	24.82	1,199.23	132.77
15	455.00	455.00	130.00	130.00	25.20	0.00	0.00	0.00	0.00	0.00	**25.64**	9.70	20.74	1,195.20	136.80
16	455.00	346.21	130.00	130.00	25.00	0.00	0.00	0.00	0.00	0.00	**63.75**	12.92	14.62	1,086.21	245.79
17	455.00	298.01	130.00	130.00	25.00	0.00	0.00	0.00	0.00	0.00	**63.51**	0.00	25.50	1,038.01	293.99
18	455.00	404.71	130.00	130.00	25.00	0.00	0.00	0.00	0.00	0.00	**63.75**	0.00	19.04	1,144.71	187.29
19	455.00	455.00	130.00	130.00	33.22	0.00	0.00	0.00	0.00	0.00	**28.72**	0.00	25.50	1,203.22	128.78
20	455.00	455.00	130.00	130.00	118.23	20.00	**0.00**	10.00	0.00	0.00	**-63.75**	0.00	18.02	1,318.23	148.77
21	455.00	450.75	130.00	130.00	25.00	20.00	**0.00**	0.00	0.00	0.00	**-63.75**	0.00	25.50	1,210.75	201.25
22	455.00	455.00	0.00	**130.00**	70.94	20.00	**0.00**	0.00	0.00	0.00	**52.36**	0.00	21.42	1,130.94	151.06
23	455.00	455.00	0.00	0.00	**53.75**	**0.00**	0.00	0.00	0.00	0.00	**63.75**	0.00	0.00	963.75	108.25
24	455.00	381.20	0.00	0.00	**25.00**	0.00	0.00	0.00	0.00	0.00	**63.75**	0.00	2.55	861.20	210.80
Total economic cost (545,294 $/day)															

The results in Table 10 reveal that the expensive units U6-U8 are successfully avoided to commit or their commitments are largely reduced compared with Table 4 due to significant discharging power support from the PEVs during the peak hours 9:00 to 14:00 and the power output from the REG. The off-peak time from 1:00 to 8:00 and 22:00-24:00 are allocated for PEVs to guarantee the overall supply of 411MW expected power for PEVs to satisfy the daily transportation necessity. It is also worth to note that the sub-peak hour 20:00 and sub-off-peak hours 16:00-18:00 are scheduled with remarkable charging and discharging power as well.

5.2.3 Case study 2-2, 0MW PEV expected power

In this case study, it is assumed that the expected power P_{exp} is 0MW, where the daily commuting power necessity is provided by REG or other resources. It is an ideal situation and will become more and more popular to only charge PEVs from the renewable power, instead of charging PEVs from thermal units. Given the same simulation data settings, the proposed PSH method is compared with a GA-LR method in [44] where there is no REG, and with a binary PSO associated by integer PSO approach in [46] where REG is presented. The numerical results of 10 independent runs with 20 particles per population and 200 iterations are shown in Table 11.

Table 11.
Numerical results for HUC considering DSLSM of PEVs (0MW) and REG

Scenarios of spinning reserve		GA-LR [44] ($/day)			BPSO+IPSO [46] Cost ($/day)	PSH Cost ($/day)				
		Best	Worst	Mean		Best	Worst	Mean	SD	CT (s)
0 MW E_{exp}	S1:with REG	—	—	—	551,977	536,440	537,367	536,758	263	48.2
	S2:without REG	561,821	566,281	564,050	—	556,360	556,981	556,646	397	47.5

It is clear from Table 11 that the proposed PSH method significantly outperformed GA-LR and BPSO+IPSO. The lower economic cost obtained by the proposed method is remarkably 15,537$ less accounting for 2.8% cost reduction compared with result optimised by the BPSO+IPSO method. Similar results were achieved in the comparison with GA-LR, where 5,461$ are saved in a day-ahead unit schedule. Moreover, the LSDSM scheduling of PEVs successfully reduced the cost by 7,577$ by comparing the best result of S2 with the optimal result of 563,937$ in case 1. The best scheduling result of S1 is shown in Table 12.

Table 12.
Best unit scheduling result of 0WM PEV load achieved by PSH method

Hour	U1 (MW)	U2 (MW)	U3 (MW)	U4 (MW)	U5 (MW)	U6 (MW)	U7 (MW)	U8 (MW)	U9 (MW)	U10 (MW)	G2V/V2G (MW)	Solar (MW)	Wind (MW)	Demand (MW)	Power reserve (MW)
1	455.00	298.21	0.00	0.00	0.00	0.00	0.00	0.00	0.00	0.00	**63.75**	0.00	10.54	753.21	167.33
2	455.00	336.48	0.00	0.00	0.00	0.00	0.00	0.00	0.00	0.00	**63.75**	0.00	22.27	791.48	140.79
3	455.00	370.21	0.00	0.00	0.00	0.00	0.00	0.00	0.00	0.00	**0.71**	0.00	25.50	825.21	110.29
4	455.00	455.00	0.00	0.00	31.79	0.00	0.00	0.00	0.00	0.00	**17.29**	0.00	25.50	941.79	155.71
5	455.00	414.83	0.00	130.00	25.00	0.00	0.00	0.00	0.00	0.00	**50.33**	0.00	25.50	1,024.83	202.67
6	455.00	455.00	0.00	130.00	35.44	0.00	0.00	0.00	0.00	0.00	**0.94**	0.00	25.50	1,075.44	152.06
7	455.00	446.92	130.00	130.00	25.00	0.00	0.00	0.00	0.00	0.00	**62.51**	0.09	25.50	1,186.92	170.67
8	455.00	455.00	130.00	130.00	40.06	0.00	0.00	0.00	0.00	0.00	**53.02**	17.46	25.50	1,210.06	164.90
9	455.00	439.30	130.00	130.00	25.00	0.00	0.00	0.00	0.00	0.00	**-63.75**	31.45	25.50	1,179.30	209.65
10	455.00	455.00	130.00	130.00	79.74	0.00	25.00	0.00	0.00	0.00	**-63.75**	36.01	25.50	1,274.74	203.77
11	455.00	455.00	130.00	130.00	107.69	20.00	25.00	0.00	0.00	0.00	**-63.75**	38.06	25.50	1,322.69	237.87
12	455.00	455.00	130.00	130.00	149.82	20.00	25.00	10.00	0.00	0.00	**-63.75**	35.93	25.50	1,374.82	238.61
13	455.00	455.00	130.00	130.00	83.97	20.00	0.00	0.00	0.00	0.00	**-63.75**	36.78	25.50	1,273.97	200.31
14	455.00	439.84	130.00	130.00	25.00	0.00	0.00	0.00	0.00	0.00	**-63.75**	31.59	24.82	1,179.84	208.57
15	455.00	444.36	130.00	130.00	25.00	0.00	0.00	0.00	0.00	0.00	**14.80**	9.70	20.74	1,184.36	178.08
16	455.00	343.48	130.00	130.00	25.00	0.00	0.00	0.00	0.00	0.00	**61.02**	12.92	14.62	1,083.48	276.06
17	455.00	294.53	130.00	130.00	25.00	0.00	0.00	0.00	0.00	0.00	**60.03**	0.00	25.50	1,034.53	322.97
18	455.00	403.55	130.00	130.00	25.00	0.00	0.00	0.00	0.00	0.00	**62.59**	0.00	19.04	1,143.55	207.49
19	455.00	397.07	130.00	130.00	25.00	0.00	0.00	0.00	0.00	0.00	**-37.43**	0.00	25.50	1,137.07	220.43
20	455.00	455.00	130.00	130.00	118.23	20.00	0.00	10.00	0.00	0.00	**-63.75**	0.00	18.02	1,318.23	166.79
21	455.00	450.75	130.00	130.00	25.00	20.00	0.00	0.00	0.00	0.00	**-63.75**	0.00	25.50	1,210.75	226.75
22	455.00	455.00	0.00	0.00	103.99	20.00	0.00	0.00	0.00	0.00	**-44.59**	0.00	21.42	1,033.99	139.43
23	455.00	455.00	0.00	0.00	46.88	0.00	0.00	0.00	0.00	0.00	**56.88**	0.00	0.00	956.88	115.12
24	455.00	366.84	0.00	0.00	0.00	0.00	0.00	0.00	0.00	0.00	**24.39**	0.00	2.55	821.84	90.71

Total economic cost (536,440 $/day)

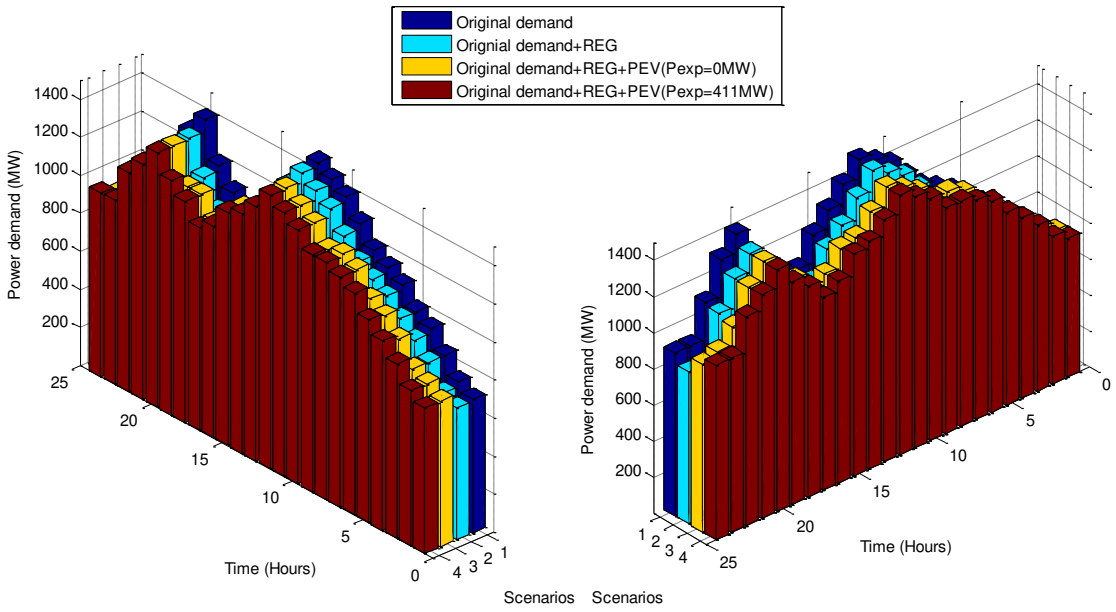

Figure 11. Accumulated power demand comparison of four HUC cases

Unsurprisingly as shown in Table 12, the commitment of expensive units U6-U10 were again largely reduced, and only one unit was extra committed (U5 at 23:00) to compensate the valley filling load from LSDSM of PEVs. Figure 11 illustrates the accumulated power demand with REG and different power expected for PEVs. It is clear that the proposed algorithm has intelligently scheduled the charging loads at both off-peak and sub-off-peak hours, and dispatched the power discharging of PEVs at peak hours, which successfully achieved the smart load shifting using demand side management of PEVs.

As a result, the proposed algorithm solves the new HUC in an effective way that the unit commitment of thermal power plants and the scheduling of charging and discharging for PEVs are simultaneously determined, with the integration of REG. The online periods of expensive units are significantly reduced, and a remarkable fossil fuel cost has been saved. A more comprehensive study in more scenarios of REGs and flexible PEVs could be found in [80].

6. Conclusion

In this paper, a new HUC model is developed which combines the traditional UC model and the integration of deterministic REG and intelligent LSDSM of PEVs. A novel PSH algorithm is proposed for solving the large scale

constrained mixed-integer HUC problem. The algorithm is a parallel-series implementation of state-of-the-art particle based methods including HTBPSO and SaDE as well as the lambda iteration. The superior performance of the new algorithm is first validated in the conventional day-ahead 10-unit power system that the proposed algorithm converged within 200 iterations and the results are stable in 30 trials. This algorithm is then applied to the HUC cases where a deterministic scenario of REG and smart charging and discharging scheduling of PEVs are both integrated. The demand side management of PEVs are conducted by allocating powers according to the proposed novel priority list of PEVs. Comparatively study shows that the proposed algorithm, once proper tuned, effectively saved 2.8% of the cost in the HUC problem with a deterministic scenario of REG and smart management of PEVs.

Future work will be addressed on employing stochastic scenarios generation methods for integrating uncertainty renewable generations into HUC problem solving, and the economic cost function may further include bidirectional power flow from PEVs and the degradation of PEV batteries. The hybrid computational tool proposed by this paper could also be extended to solve unit commitment integrating with other dispatchable load types such as energy storages and virtual power plants for smart demand side management.

Acknowledgement

This work was financially supported by UK EPSRC under grant EP/L001063/1 and China NSFC under grants 61673256, 61273040, 51607177 and 61533010. Zhile Yang would like to thank EPSRC Studentship for financially supporting on his research.

Reference

[1] N. Padhy. Unit commitment-a bibliographical survey. Power Systems, IEEE Transactions on, 2004, 19(2): 1196-1205.

[2] G. Os´orio, J. Lujano-Rojas, J. Matias, J. Catal˜ao, A new scenario generation-based method to solve the unit commitment problem with high penetration of renewable energies, International Journal of Electrical Power & Energy Systems 64 (2015) 1063–1072.

[3] S. Moradi, S. Khanmohammadi, M. Hagh, B. Mohammadi-ivatloo. A semi-analytical non-iterative primary approach based on priority list to solve unit commitment problem. Energy, 2015, 88: 244-259.

[4] J. López, J. Ceciliano-Meza, I. Guillén, R. Gómez. A Heuristic algorithm to solve the unit commitment problem for real-life large-scale power systems. International Journal of Electrical Power & Energy Systems, 2013, 49: 287-295.

[5] J. Alemany, F. Magnago, D. Moitre, H. Pinto, Symmetry issues in mixed integer programming based unit commitment, International Journal of Electrical Power & Energy Systems 54 (2014) 86–90.

[6] Q. Jiang, B. Zhou, M. Zhang, Parallel augment Lagrangian Relaxation method for transient stability constrained unit commitment, Power Systems, IEEE Transactions on 28 (2) (2013) 1140–1148.

[7] H. Ma, D. Simon, M. Fei and Z. Chen, On the equivalences and differences of evolutionary algorithms. Engineering Applications of Artificial Intelligence, 2013, 26(10): 2397-2407.

[8] H. Ma, D. Simon, M. Fei, X. Shu, Z. Chen. Hybrid biogeography-based evolutionary algorithms. Engineering Applications of Artificial Intelligence, 2014, 30: 213-224.

[9] B. Garl´ık, M. K˘rivan, Renewable energy unit commitment, with different acceptance of balanced power, solved by simulated annealing, Energy and Buildings 67 (2013) 392–402.

[10] A. Kazarlis, A. Bakirtzis, V. Petridis, A genetic algorithm solution to the unit commitment problem, Power Systems, IEEE Transactions on 11 (1) (1996) 83–92.

[11] H. Quan, D. Srinivasan, A. Khosravi. Integration of renewable generation uncertainties into stochastic unit commitment considering reserve and risk: A comparative study. Energy, 2016, 103: 735-745.

[12] X. Yuan, H. Nie, A. Su, L. Wang, Y. Yuan, An improved binary particle swarm optimization for unit commitment problem, Expert Systems with applications 36 (4) (2009) 8049–8055.

[13] Y. Jeong, J. Park, S. Jang, K. Lee. A new quantum-inspired binary PSO: application to unit commitment problems for power systems. Power Systems, IEEE Transactions on, 2010, 25(3): 1486-1495.

[14] B. Ji, X. Yuan, Z. Chen, H. Tian, Improved gravitational search algorithm for unit commitment considering uncertainty of wind power, Energy 67 (2014) 52–62.

[15] B. Saravanan, E. Vasudevan, D. Kothari. Unit commitment problem solution using invasive weed optimization algorithm. International Journal of Electrical Power & Energy Systems, 55 (2014): 21-28.

[16] X. Zhang, T. Yu, B. Yang, L. Cheng, Accelerating bio-inspired optimizer with transfer reinforcement learning for reactive power optimization, Knowledge-Based Systems (2016), http://dx.doi.org/10.1016/j.knosys. 2016.10.024

[17] P. Attaviriyanupap, H. Kita, E. Tanaka, J. Hasegawa, A hybrid LR-EP for solving new profit-based UC problem under competitive environment, Power Systems, IEEE Transactions on 18 (1) (2003) 229–237.

[18] T. Logenthiran, W. Woo, V. Phan, Lagrangian Relaxation hybrid with evolutionary algorithm for short-term generation scheduling, International Journal of Electrical Power & Energy Systems 64 (2015) 356–364.

[19] A. Y. Saber, G. K. Venayagamoorthy, Intelligent unit commitment with vehicle-to-grid a cost-emission optimization, Journal of Power Sources 195 (3) (2010) 898–911.

[20] J. Zhang, Q. Tang, Y. Chen, S. Lin. A hybrid particle swarm optimization with small population size to solve the optimal short-term hydro-thermal unit commitment problem. Energy, 2016, 109: 765-780.

[21] T. Lau, C. Chung, K. Wong, T. Chung, S. Ho, Quantum-inspired evolutionary algorithm approach for unit commitment, Power Systems, IEEE Transactions on 24 (3) (2009) 1503–1512.

[22] B. Ji, X. Yuan, X. Li, Y. Huang, W. Li, Application of quantum-inspired binary gravitational search algorithm for thermal unit commitment with wind power integration, Energy Conversion and Management 87 (2014) 589–598.

[23] Y. Li, L. Jiang, Q. Hu, P. Wang et al., Wind-thermal power system dispatch using MLSAD model and GSOICLW algorithm, Knowledge Based Systems (2016), http://dx.doi.org/10.1016/j.knosys.2016.10.028

[24] X. Hu, S. Moura, N. Murgovski, B. Egardt, D. Cao. Integrated optimization of battery sizing, charging, and power management in plug-in hybrid electric vehicles. IEEE Transactions on Control Systems Technology, 2016, 24(3): 1036-1043.

[25] F. Mwasilu, J. Justo, E. Kim, T. Do, J. Jung, Electric vehicles and smart grid interaction: A review on vehicle to grid and renewable energy sources integration, Renewable and Sustainable Energy Reviews 34 (2014) 501–516.

[26] United nations conference on climate change, [Online]. <http://www.cop21.gouv.fr/en/learn/> (Accessed on Jan 2016)

[27] C. Chan, The state of the art of electric, hybrid, and fuel cell vehicles, Proceedings of the IEEE 95 (4) (2007) 704–718.

[28] Z. Yang, K. Li, A. Foley. Computational scheduling methods for integrating plug-in electric vehicles with power systems: A review. Renewable and Sustainable Energy Reviews, 2015, 51: 396-416.

[29] J. Hu, H. Morais, T. Sousa, M. Lind. Electric vehicle fleet management in smart grids: A review of services, optimization and control aspects. Renewable and Sustainable Energy Reviews, 2016, 56: 1207-1226.

[30] Kempton W, Tomić J. Vehicle-to-grid power fundamentals: Calculating capacity and net revenue. Journal of power sources, 2005, 144(1): 268-279.

[31] S. Han, S. Han, K. Sezaki, Development of an optimal vehicle-to-grid aggregator for frequency regulation. Smart Grid, IEEE Transactions on, 2010, 1(1): 65-72.

[32] M. Honarmand, A. Zakariazadeh, S. Jadid, Integrated scheduling of renewable generation and electric vehicles parking lot in a smart microgrid. Energy Conversion and Management, 2014, 86: 745-755.

[33] M. Ghofrani, A. Arabali, M. Etezadi-Amoli, M. Fadali, Smart scheduling and Cost-Benefit analysis of Grid-Enabled electric vehicles for wind power integration. Smart Grid, IEEE Transactions on, 2014, 5(5): 2306-2313.

[34] T. Wu, Q. Yang, Z. Bao, W. Yan, Coordinated energy dispatching in microgrid with wind power generation and plug-in electric vehicles, Smart Grid, IEEE Transactions on, 2013, 4(3): 1453-1463.

[35] Q. Huang, Q. Jia, Z. Qiu, G. Deconinck , Matching EV Charging Load With Uncertain Wind: A Simulation-Based Policy Improvement Approach, Smart Grid, IEEE Transactions on, 2015, 6(3): 1425-1433

[36] X. Hu, C. Martinez, Y. Yang. Charging, power management, and battery degradation mitigation in plug-in hybrid electric vehicles: a unified cost-optimal approach. Mechanical Systems and Signal Processing, 2017, 87: 4-16.

[37] X. Hu, Y. Zou, Y. Yang. Greener plug-in hybrid electric vehicles incorporating renewable energy and rapid system optimization. Energy, 2016, 111: 971-980.

[38] L. Li, S. You, C. Yang, B. Yan, J. Song, Z. Chen, Driving-behavior-aware stochastic model predictive control for plug-in hybrid electric buses. Applied Energy,2016: 162, 868-879.

[39] L. Li, B. Yan, C. Yang, Y. Zhang, Z. Chen, G. Jiang, Application-Oriented Stochastic Energy Management for Plug-in Hybrid Electric Bus With AMT. IEEE Transactions on Vehicular Technology, 2016, 65(6): 4459-4470.

[40] X. Zhang, S. E. Li, H. Peng, J. Sun, Efficient exhaustive search of power-split hybrid powertrains with multiple planetary gears and clutches. Journal of Dynamic Systems, Measurement, and Control, 2015, 137(12): 121006.

[41] X. Zhang, S. E. Li, H. Peng, J. Sun, Design of Multimode Power-Split Hybrid Vehicles—A Case Study on the Voltec Powertrain System[J]. IEEE Transactions on Vehicular Technology, 2016, 65(6): 4790-4801.

[42] Z. Yang, K. Li, Q. Niu, Y. Xue, A. Foley, A self-learning TLBO based dynamic economic/environmental dispatch considering multiple plug-in electric vehicle loads, Journal of Modern Power Systems and Clean Energy (2014) 1–10.

[43] A. Saber, G. Venayagamoorthy, Intelligent unit commitment with vehicle-to-grid a cost-emission optimization, Journal of Power Sources 195 (3) (2010) 898–911.

[44] E. Talebizadeh, M. Rashidinejad, A. Abdollahi, Evaluation of plug-in electric vehicles impact on cost-based unit commitment, Journal of Power Sources 248 (2014) 545–552.

[45] A. Saber, G. Venayagamoorthy, Efficient utilization of renewable energy sources by gridable vehicles in cyber-physical energy systems, Systems Journal, IEEE, 2010, 4(3): 285-294.

[46] A. Saber, G. Venayagamoorthy, Plug-in vehicles and renewable energy sources for cost and emission reductions, Industrial Electronics, IEEE Transactions on, 2011, 58(4): 1229-1238.

[47] P. Palensky, D. Dietrich. Demand side management: Demand response, intelligent energy systems, and smart loads. Industrial Informatics, IEEE Transactions on, 2011, 7(3): 381-388.

[48] B. Zhou, T. Littler, L. Meegahapola, H. Zhang. Power system steady-state analysis with large-scale electric vehicle integration. Energy, 2016, 115: 289-302.

[49] J. García-Villalobos, I. Zamora, JI. San Martín, F. Asensio, V. Aperribay. Plug-in electric vehicles in electric distribution networks: A review of smart charging approaches. Renewable and Sustainable Energy Reviews, 2014, 38: 717-731.

[50] Q. Niu, H. Zhang, K. Li, G. W. Irwin, An efficient harmony search with new pitch adjustment for dynamic economic dispatch, Energy, 65 (2014) 25–43.

[51] X. Li, J. Cao, D. Du. Probabilistic optimal power flow for power systems considering wind uncertainty and load correlation. Neurocomputing, 2015, 148: 240-247.

[52] J. Kennedy, R. C. Eberhart, A discrete binary version of the particle swarm algorithm, in: Systems, Man, and Cybernetics, 1997. Computational Cybernetics and Simulation. 1997 IEEE International Conference on, Vol. 5, IEEE, 1997, pp. 4104–4108.

[53] Z. Gaing, Discrete particle swarm optimization algorithm for unit commitment, in: Power Engineering Society General Meeting, 2003, IEEE, Vol. 1, IEEE, 2003.

[54] H. Nezamabadi-pour, M. Rostami Shahrbabaki, M. Maghfoori-Farsangi, Binary particle swarm optimization: challenges and new solutions, CSI J Comput Sci Eng 6 (1) (2008) 21–32.

[55] L. Wang, X. Wang, J. Fu, L. Zhen, A novel probability binary particle swarm optimization algorithm and its application, Journal of software 3 (9) (2008) 28–35.

[56] Z. Beheshti, S. M. Shamsuddin, S. Hasan, Memetic binary particle swarm optimization for discrete optimization problems, Information Sciences 299 (2015) 58–84.

[57] Q. Shen, J.-H. Jiang, C.-X. Jiao, G.-l. Shen, R.-Q. Yu, Modified particle swarm optimization algorithm for variable selection in MLR and PLS modeling: Qsar studies of antagonism of angiotensin ii antagonists, European Journal of Pharmaceutical Sciences 22 (2) (2004) 145–152.

[58] F. Afshinmanesh, A. Marandi, A. Rahimi-Kian, A novel binary particle swarm optimization method using artificial immune system, in: Computer as a Tool, 2005. EUROCON 2005. The International Conference on, Vol. 1, IEEE, 2005, pp. 217–220.

[59] M. A. Khanesar, M. Teshnehlab, M. A. Shoorehdeli, A novel binary particle swarm optimization, in: Control & Automation, 2007. MED'07. Mediterranean Conference on, IEEE, 2007, pp. 1–6.

[60] S. Pookpunt,W. Ongsakul, Optimal placement of wind turbines within wind farm using binary particle swarm optimization with time-varying acceleration coefficients, Renewable Energy 55 (2013) 266–276.

[61] D. Tang, Y. Cai, J. Zhao, Y. Xue, A quantum-behaved particle swarm optimization with memetic algorithm and memory for continuous non-linear large scale problems, Information Sciences 289 (2014) 162–189.

[62] J. Brest, S. Greiner, B. Boskovic, M. Mernik, and V. Zumer, Self-adapting control parameters in differential evolution: a comparative study on numerical benchmark problems, Evolutionary Computation, IEEE Transactions on, 2006, 10(6): 646-657.

[63] Z. Yang, J. He, X. Yao, Making a Difference to Differential Evolution, in Advances in Meta-heuristics for Hard Optimization, New York: Springer-Verlag, 2007, pp. 415–432

[64] A. Qin, V. Huang, P. Suganthan. Differential evolution algorithm with strategy adaptation for global numerical optimization. Evolutionary Computation, IEEE Transactions on, 2009, 13(2): 398-417.

[65] J. Zhang, A. Sanderson, JADE: adaptive differential evolution with optional external archive. Evolutionary Computation, IEEE Transactions on, 2009, 13(5): 945-958.

[66] S. Das, A. Abraham, U. Chakraborty, A Konar, Differential evolution using a neighbourhood-based mutation operator, Evolutionary Computation, IEEE Transactions on, 2009, 13(3): 526-553.

[67] T. Ting, M. Rao, C. Loo, A novel approach for unit commitment problem via an effective hybrid particle swarm optimization, Power Systems, IEEE Transactions on 21 (1) (2006) 411–418.

[68] B. Zhao, C. Guo, B. Bai, Y. Cao, An improved particle swarm optimization algorithm for unit commitment, International Journal of Electrical Power & Energy Systems 28 (7) (2006) 482–490.

[69] K. Chandrasekaran, S. P. Simon, Network and reliability constrained unit commitment problem using binary real coded firefly algorithm, International Journal of Electrical Power & Energy Systems 43 (1) (2012) 921–932.

[70] X. Yu, X. Zhang, Unit commitment using Lagrangian Relaxation and particle swarm optimization, International Journal of Electrical Power & Energy Systems 61 (2014) 510–522.

[71] X. Yuan, B. Ji, S. Zhang, H. Tian, Y. Hou, A new approach for unit commitment problem via binary gravitational search algorithm, Applied Soft Computing 22 (2014) 249–260.

[72] A. Shukla, S. Singh. Advanced three-stage pseudo-inspired weight-improved crazy particle swarm optimization for unit commitment problem. Energy, 2016, 96: 23-36.

[73] V. Pappala, I, Erlich, A new approach for solving the unit commitment problem by adaptive particle swarm optimization, Power and Energy Society general meeting-conversion and delivery of electrical energy in the 21st century. 2008, IEEE, USA, pp 1–6

[74] A. Eldin, M. El-sayed, H. Youssef, A two-stage genetic based technique for the unit commitment optimization problem. In: 12th International middle east power system conference, MEPCO 2008, Aswan, pp 425–430

[75] W. Xiong, M. Li, Y. Cheng, An improved particle swarm optimization algorithm for unit commitment. In: Proceedings of the 2008 international conference on intelligent computation technology and automation, vol 01, pp 21–25

[76] S. Khanmohammadi, M. Amiri, M. Haque. A new three-stage method for solving unit commitment problem. Energy, 2010, 35(7): 3072-3080.

[77] V. Kamboj, S. Bath, J. Dhillon. Hybrid HS–random search algorithm considering ensemble and pitch violation for unit commitment problem. Neural Computing and Applications, 1-26.

[78] U.S. DOT, National Household Travel Survey <http://nhts.ornl.gov/>

[79] A. Qin, P. Suganthan, Self-adaptive differential evolution algorithm for numerical optimization, Evolutionary Computation, 2005, IEEE Congress on. IEEE, 2005, 2: 1785-1791.

[80] Z. Yang, K. Li, Q. Niu, Y. Xue. A comprehensive study of economic unit commitment of power systems integrating various renewable generations and plug-in electric vehicles. Energy Conversion and Management, 2017, 132: 460-481.